AD-A127 023 ANALYSIS OF NOAA/ALASKAN MST RADAR DATA(U) CORNELL UNIV 1/1
ITHACA NY DEPT OF ELECTRICAL ENGINEERING
M F LARSEN ET AL. NOV 82 AFOSR-TR-83-0236 AFOSR-80-0020
UNCLASSIFIED F/G 17/9 NL

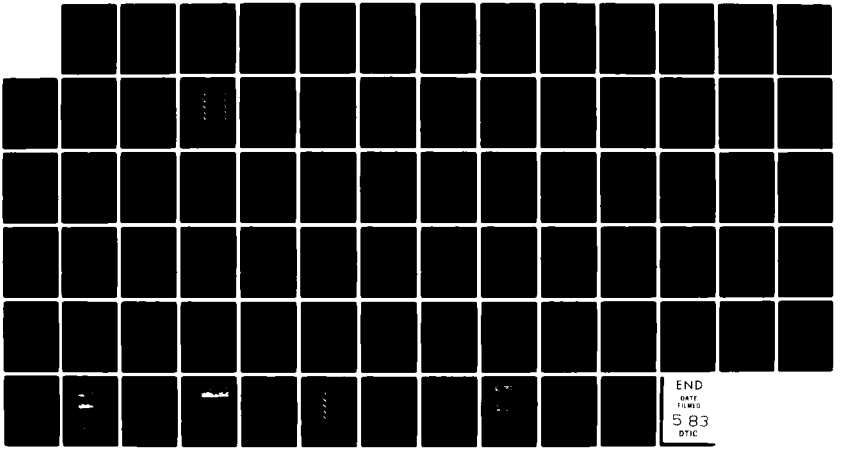

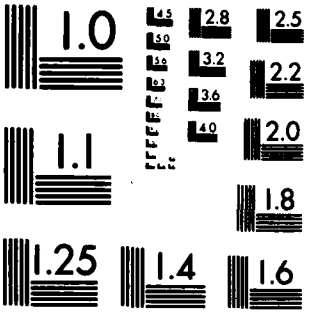

MICROCOPY RESOLUTION TEST CHART
NATIONAL BUREAU OF STANDARDS-1963-A

UNCLASSIFIED

SECURITY CLASSIFICATION OF THIS PAGE (When Data Entered)

REPORT DOCUMENTATION PAGE	READ INSTRUCTIONS BEFORE COMPLETING FORM
1. REPORT NUMBER AFOSR-TR- 83-0236	2. GOVT ACCESSION NO. A127023
	3. RECIPIENT'S CATALOG NUMBER
4. TITLE (and Subtitle) ANALYSIS OF NOAA/ALASKAN MST RADAR DATA	5. TYPE OF REPORT & PERIOD COVERED Final Report
	6. PERFORMING ORG. REPORT NUMBER
7. AUTHOR(s) M. F. Larsen, M. C. Kelley, D. T. Farley	8. CONTRACT OR GRANT NUMBER(s) AFOSR-80-0020
9. PERFORMING ORGANIZATION NAME AND ADDRESS Cornell University, Electrical Engineering Dept. Ithaca, N.Y. 14853	10. PROGRAM ELEMENT, PROJECT, TASK AREA & WORK UNIT NUMBERS 61102F 2310/A1
11. CONTROLLING OFFICE NAME AND ADDRESS Air Force Office of Scientific Research/NC Bolling AFB, DC 20332	12. REPORT DATE November 1982
	13. NUMBER OF PAGES 78
14. MONITORING AGENCY NAME & ADDRESS(if different from Controlling Office)	15. SECURITY CLASS (of this report) Unclassified
	15a. DECLASSIFICATION DOWNGRADING SCHEDULE

16. DISTRIBUTION STATEMENT (of this Report)

Approved for public release;
distribution unlimited.

17. DISTRIBUTION STATEMENT (of the abstract entered in Block 20, if different from Report)

18. SUPPLEMENTARY NOTES

APR 21 1983

A

19. KEY WORDS (Continue on reverse side if necessary and identify by block number)

MST Radar	Geostrophic Balance
Poker Flat Radar	Turbulence Spectra
Mesoscale Turbulence	Atmospheric Turbulence

20. ABSTRACT (Continue on reverse side if necessary and identify by block number)

Beginning in 1979 Cornell University was funded for the purpose of analyzing the high time-resolution measurements provided by the Poker Flat VHF Doppler radar. The research emphasized applications of the technique to investigations of synoptic and mesoscale dynamics. The primary research areas included determining the characteristics of mesoscale turbulence in the range of periods from a few hours to several days and determining the extent to which the geostrophic balance condition is satisfied at time scales of a day or less.

DD FORM 1 JAN 73 1473

UNCLASSIFIED

SECURITY CLASSIFICATION OF THIS PAGE (When Data Entered)

DTIC FILE COPY

AFOSR-TR- 83-0236

Final Scientific Report

ANALYSIS OF NOAA/ALASKAN MST RADAR DATA

(AFOSR-80-0020)

M.F. Larsen

M.C. Kelley

D.T. Farley

November 1982

Abstract

Beginning in 1979 Cornell University was funded for the purpose of analyzing the high time-resolution measurements provided by the Poker Flat VHF Doppler radar. The research emphasized applications of the technique to investigations of synoptic and mesoscale dynamics. The primary research areas included determining the characteristics of mesoscale turbulence in the range of periods from a few hours to several days and determining the extent to which the geostrophic balance condition is satisfied at time scales of a day or less.

1. Introduction

The Poker Flat, Alaska MST (Mesosphere-Stratosphere-Troposphere) radar has been a rich source of wind data of a type never seen before. The height range covered and the time resolution of the measurements have made it possible to explore important topics in atmospheric dynamics about which little was known. Cornell was funded in 1979 for the purpose of aiding in the analysis of the wind data that was just becoming available in the beginning of that year. A number of other investigators have also been involved in utilizing the radar measurements as part of their research programs, but our particular emphasis was on the synoptic applications of the research tool.

Even though a number of investigators have been involved in analyzing data from the MST radar, only the surface of the data base has been scratched. That is certainly true in the area of synoptic and mesoscale dynamics. Since no previous work had been done with long time series of high resolution wind data such as these, our studies involved investigations of the most basic character of the dynamics. Turbulence spectra at periods characteristic of the mesoscale were calculated, and the results were found to have some important consequences in terms of the direction of energy flow along the spectrum (see Appendix I). We concluded that further investigations in this area should be carried out since basic questions of the predictability of mesoscale flows will depend on the results. The second part of the investigation was the most involved. The degree to which the geostrophic balance condition is satisfied was tested using 40 days of radar data and radiosonde data from the five

radiosonde stations nearest the location of the radar (see Appendix II). Geostrophy is of interest both from the point of view of understanding the dynamics of the flow, and from the point of view of testing the various objective analysis or data assimilation schemes that are used to initialize numerical forecast models. The third part of the study involved a review paper for the Bulletin of the American Meteorological Society written by M.F. Larsen from Cornell and J. Rottger from the Max-Planck-Institut fur Aeronomie (see Appendix III). The review was deemed to be important since it brought together previous results that were scattered in the literature in a wide variety of journals, many of which are not readily accessible to the meteorological community and summarized the present state of synoptic and mesoscale research using VHF and UHF Doppler radars.

2. Mesoscale turbulence spectra

Forty days of radar wind data from the end of February to the beginning of April 1979 were used to investigate turbulence at the meteorological mesoscale. The radar data was taken with a time resolution of 4 min using two beams pointing 15° off vertical. It was assumed that the entire contribution to the line-of-sight velocities was from the horizontal wind components since no information on the vertical winds was available at that time. The 4-min data were averaged to produce hourly values in order to minimize any contamination due to large vertical velocities that occur occasionally. The time series then consisted of 40 days of 1-hour average winds at six heights

between 3.79-km and 14.79-km altitude. Very little is known about the dynamics at these time scales.

The turbulence spectra over the height range studied were found to follow a -5/3 spectral power slope at periods from a few days to a few hours (actually -1.602 ± 0.250). If the Taylor hypothesis holds and the turbulence is frozen into the fluid, the frequency and wavenumber spectra will be related by a constant of proportionality given by the mean wind over the time period sampled. The -5/3 wavenumber spectrum implies one of two things. It may be associated with the energy cascading inertial subrange of two-dimensional turbulence (Gage, 1979) or with a spectrum of buoyancy waves (Dewan, 1979). Since the energy flow in two-dimensional turbulence is constrained to be from small to large scales, the former possibility implies that there is an energy source at large wavenumbers (small horizontal scales) cascading energy toward larger scales. The implication would be that initial data at very small scales would be needed in order to predict the evolution of the flow at slightly larger scales in the mesoscale range. In the second case the spectrum is characterized by essentially three-dimensional "turbulence" associated with strongly interacting buoyancy waves. Most of what is known about this type of spectrum derives from observations of ocean waves and is generally referred to as the empirical Garrett-Munk spectrum. Studies of the energy cascade for this type of spectrum in the ocean indicate that the flow is most likely from large to small scales (LeBlond and Mysak, 1980). The results of this part of our study are described in detail in Larsen et al. (1982) reproduced in Appendix I.

The essential characteristic difference between the two types of

turbulence is in the spectrum of the vertical variations. The Garrett-Munk spectrum has a -2.5 vertical wavenumber spectral slope while two-dimensional turbulence is not expected to have any consistent slope. We could not decide which was the correct interpretation based on the data available from Poker Flat since there were only 6 data points in the troposphere and lower stratosphere. It would be possible to resolve the question using data with a height resolution of 150 m, something that is easily achievable. The consequences of the result are important enough that further investigation is warranted.

3. Geostrophy and objective analysis

Very little is known about the balance conditions in the atmosphere except at very long time scales (see e.g., Errico, 1982). The pressure and temperature data provided by the standard National Weather Service radiosondes are generally of good enough quality to assess the balance, but the errors in the wind data are too large. For example, Bengtsson et al. (1982) estimated the error to be approximately 6 m/s above 600 mb. However, the radar wind data is high quality data with sufficiently small errors to test the balance conditions. Also, the high time-resolution data can be averaged in time to get a better estimate of the wind appropriate for a given time scale.

The balance conditions are important both in terms of the dynamics of the synoptic and mesoscale flow, and also in terms of the objective analysis schemes that are used routinely to initialize numerical models for research and

forecasting purposes. Most objective analysis schemes are now multivariate, utilizing both wind and geopotential height data in deriving the grid of objectively analyzed values. The goal is to produce a grid of input values that are free from meteorological noise and are compatible with the model dynamics. The simplest balance condition used to relate heights and winds is the geostrophic approximation.

It has been difficult to test the geostrophic balance due to the poor quality of the balloon wind measurements. We used 40 days of 1-hour average radar data and radiosonde data from the five nearest radiosonde stations to test the balance. The geostrophic wind was calculated from the grid of geopotential height values found by applying the Cressman univariate objective analysis scheme to the raw data. The radar measurements were then compared to the geostrophic wind. The radar winds and the rawinsonde winds were also compared in order to provide an independent estimate of the accuracy of the rawinsonde measurement. The root-mean-square difference between the two independent wind measurements was found to be 3 to 4 m/s, somewhat better than the estimate of 6 m/s by Bengtsson et al. (1982). The error decreased to 2 to 3 m/s when the averaging interval for the radar data was increased to 24 hours. We also found that the r.m.s. difference between the radar and geostrophic winds and the rawinsonde and geostrophic winds was 1.5 to 2.0 m/s greater than the difference between the two wind measurements. The relationship held true even when the averaging interval was increased from 1 hour to 24 hours. Thus, the ageostrophic wind component for time scales of 24 hours or less was of the order of 1.5 to 2.0 m/s.

The objective analysis schemes that use the geostrophic equation to relate measured wind data to the height fields for analysis purposes effectively assume a cross-correlation of 1.0 between the winds and height gradients at zero spatial separation. The correlations between the measured winds and the calculated geostrophic winds were also calculated. The cross-correlations for both the zonal and meridional components was found to be close to 0.75 essentially independent of height. The results of this study are described in detail in Larsen (1982) reproduced in Appendix II.

4. Status of synoptic and mesoscale VHF radar research

The literature detailing past and present research using the VHF and UHF Doppler radar technique has been scattered in a variety of journals. Although some articles have been published in meteorological journals, many have appeared in geophysical or radio research journals. With that in mind, part of the funds provided by AFOSR were used to support the writing of a review article for the Bulletin of the American Meteorological Society. The object of the review was to acquaint the meteorologist with the research applications of the radar technique for synoptic and mesoscale research. The article (Larsen and Rottger, 1982) is reproduced in full in Appendix III.

5. Recommendations for future research

The results presented here show an ambiguity about the direction of energy flow along the wavenumber spectrum in the mesoscale range. The problem

can be resolved most easily by determining the characteristics of the vertical wavenumber spectrum. The height resolution of 2.2 km used routinely at the Poker Flat radar is inadequate for this purpose, but winds measured at 150 m intervals would be useful. Such data could be provided by the Poker Flat facility during a special data-taking period or by another radar such as the Arecibo 430 MHz radar.

We have studied the geostrophy of the flow as it relates to a simple objective analysis scheme. The accuracy and time resolution of the radar technique makes it ideal for comparisons of measured and gridded values produced by the various data assimilation schemes. The test of geostrophy should be carried out for a longer time series to determine if there is any dependence on season. The radar data should also be compared to the output from a normal mode initialization scheme (Daley, 1981). This type of scheme has several advantages over the simpler schemes. The gridded values are exactly compatible with the dynamics of the numerical model, yet none of the meteorologically significant high-frequency information is lost. The normal mode initialization procedure also provides the amplitudes of both the Rossby and inertio-gravity wave components and the fast gravity wave components. A comparison of the output from such a scheme and the radar data will provide an estimate of the errors associated with various wave components and will provide a better understanding of the dynamics associated with the various errors.

References

Bengtsson, L., M. Kanamitsu, P. Kallberg, and S. Uppala, 1982: FGGE 4-dimensional data assimilation at ECMWF. Bull. Amer. Meteorol. Soc., 63, 29-43.

Daley, R., 1981: Normal mode initialization. Rev. Geophys. Space Phys., 19, 450-468.

Dewan, E.M., 1979: Stratospheric wave spectra resembling turbulence. Science, 204, 832.

Errico, M., 1982: Normal mode initialization and the generation of gravity waves by quasi-geostrophic forcing. J. Atmos. Sci., 39, 573-586.

Gage, K.S., 1979: Evidence for a $k^{-5/3}$ law inertial range in mesoscale two-dimensional turbulence. J. Atmos. Sci., 36, 1950-1954.

Larsen, M.F., M.C. Kelley, and K.S. Gage, 1982: Turbulence spectra in the upper troposphere and lower stratosphere at periods between 2 hours and 40 days. J. Atmos. Sci., 39, 1035-1041.

Larsen, M.F., and J. Rottger, 1982: VHF and UHF Doppler radars as tools for synoptic research. Bull. Amer. Meteorol. Soc., 63, 996-1008.

Larsen, M.F., 1982: Can a VHF Doppler radar provide synoptic wind data?: A comparison of 30 days of radar and radiosonde data. Submitted to Mon. Wea. Rev.

LeBlond, P.H., and L.A. Mysak, 1980: Waves in the Ocean, Elsevier North-Holland, New York, 602 pp.

APPENDIX I

Reprinted from JOURNAL OF THE ATMOSPHERIC SCIENCES, Vol. 39, No. 5, May 1982
American Meteorological Society
Printed in U. S. A.

Turbulence Spectra in the Upper Troposphere and Lower Stratosphere at Periods Between 2 Hours and 40 Days

MIGUEL FOLKMAR LARSEN AND MICHAEL C. KELLEY

Cornell University, Ithaca, NY 14850

K. S. GAGE

Aeronomy Laboratory, NOAA, Boulder, CO 80303

(Manuscript received 19 August 1981, in final form 18 January 1982)

ABSTRACT

Zonal and meridional wind measurements made with the Poker Flat MST radar over a 40-day period are used to calculate the frequency power spectra at heights between 5.99 and 14.69 km. The winds used in the analysis are 1 h averages of samples taken every 4 min. We find that the spectra follow an $f^{-5/3}$ power law in the range of periods from 2 to 50 h. If the Taylor transformation is valid in this frequency range, this would imply a $k^{-5/3}$ wavenumber spectrum, corresponding to an inertial subrange for two-dimensional turbulence at the atmospheric mesoscale. These observations support and extend earlier studies which also show a $-5/3$ power law behavior in the atmospheric mesoscale.

1. Introduction

The study of atmospheric turbulence spectra is important for two reasons. First, the shape of the spectrum shows the position of the sources and sinks of energy and enstrophy and how nonlinear interactions distribute these quantities in a statistical sense. Second, the limits of predictability of the atmospheric state depend on the form of the wavenumber power law as shown by the work of Lorenz [1969] and Leith and Kraichnan (1972). A large number of studies have been made with the aim of defining the frequency or wavenumber power laws. In general they fall into one of two categories, those dealing with large spatial and temporal scales utilizing rawinsondes (Kao and Wendell, 1970; Kao and Lee, 1977; Julian *et al.*, 1970) or superpressure balloons (Mantis, 1963; Wooldridge and Reiter, 1970; Desbois, 1975); and those dealing with small scales utilizing data from instrumented aircraft (Kao and Woods, 1964), meteorological towers or tethered balloons (Chernikov *et al.*, 1969). The part of the spectrum where little information has been available is in the atmospheric mesoscale.

The mesoscale is characterized by periods from a few tens of minutes up to a few days and spatial scales of 1000 km or less. Meteorological towers or tethered balloons are capable of resolving frequencies in this range but they cannot operate outside the planetary boundary layer. Since rawinsondes are launched twice per day, the minimum frequency that can be resolved has a period of one day. This is at the outer edge of the mesoscale range. The superpressure balloons which are flown in the Southern Hemisphere have the potential for investigating subsynoptic scale motions (see, e.g., Cadet, 1978) but until recently the temporal resolution has been on the order of a day due to problems of data storage and transmission.

The NOAA MST (Mesosphere/Stratosphere/Troposphere) radar located at Poker Flat, Alaska was put into routine operation in the first months of 1979. The system has been described in detail by Balsley *et al.* (1980), Gage and Balsley (1978) and Balsley and Gage (1980). The radar uses the Doppler shift of signals backscattered by turbulent fluctuations in the refractive index to measure line-of-sight velocities. By using three beams pointed in different directions, the complete profile of the vector winds can be determined. The time resolution is only limited by the integration time required to obtain a good signal-to-noise ratio. However, the fact that the Poker Flat radar is designed to operate unattended means that there is a practical limit imposed on the time resolution in order to avoid changing data tapes too often. For this reason the time between successive profiles is four minutes. In 1979 when the data set described here was obtained, only a quarter of the full system had been completed. Thus the altitude range in which useful measurements could be obtained was limited to heights between 5.99 and 14.79 km. The time resolution and height range covered make the instrument ideal for investigating the power spectra of motions at synoptic and mesoscales.

0022-4928/82/051035-07$05.75

2. Description of the data set and spectral analysis

During the time from 23 February to 5 April 1979 the Poker Flat radar was operated in a mode with two beams at 15° off-vertical, one pointed roughly north and the other roughly east. Computing limitations excluded the possibility of operating a third, vertically-pointing beam during that time although this situation has been rectified since then. For this original data set it was assumed that the entire contribution to the line-of-sight velocities was due to a horizontal wind vector. The antenna consisted of a 100 m^2 phased dipole array, one-fourth the size the array will have upon completion. Sixteen 100 kW transmitters were used, giving a peak transmitted power of 0.8 MW per beam. This configuration together with a 15 μs pulsewidth provided one complete profile every 4 min up to an altitude of 14.69 km and a height resolution of ~2.2 km.

Coherent integrations and the Fast Fourier Transforms of the received signals are done on line. The spectra are then processed at the Aeronomy Lab in Boulder, Colorado. The processing scheme is described in Carter *et al.* (1980) and provides line-of-sight Doppler shifts at each height. The assumption that the entire contribution to the line-of-sight velocities is due to a horizontal wind vector is an increasingly good assumption as the averaging interval is increased. One way to understand this is to consider the polarization relations for gravity waves in an isothermal atmosphere [given by Beer (1974) for instance]. The requirement for the validity of the hydrostatic approximation turns out to be that $\omega^2 \ll \omega_b^2$, where ω is the angular frequency of the motion and ω_b is the Brunt-Vaisala period. For periods of 30 min or more the contribution from the vertical velocity component is certainly negligible. However for samples taken at intervals less than this, the vertical velocity component can contribute significantly. To avoid problems of this type, the 4 min data was averaged over 1 h intervals centered on the full hour. The data thus consists of 42 days of 1 h average horizontal winds. For this study 40 of the days were used, yielding a time series of 960 points.

The time series was treated in several ways before the spectra were calculated. First, missing data points were replaced by interpolating between adjacent points. The number of missing points was <45, out of the total of 960, for the heights discussed here. Above 14.69 km and below 5.99 km data were also available, but the number of missing points was approximately four times as large. After the missing data points were replaced by the interpolated values the mean was calculated and subtracted. Then a Hanning window was applied, affecting 96 or 10% of the points at each end of the series. The Hanning window helps to eliminate energy spillage from the low frequency end of the spectrum into the high frequency end as a result of broadening due to discrete sampling.

The original data is shown in Fig. 1. The five curves at the top of the figure are for the zonal wind, and the curves at the bottom are for the meridional component. The data that are shown have not been treated in any way. Both the average for the entire time series at each height and the variance are given below the corresponding curve. Each time series was screened for occurrences of wind variations >7 m s^{-1} between adjacent points. In almost all cases where variations larger than this occurred a large change in the wind component was found both preceding and following the questionable data point. A data point such as this was considered to be erroneous and replaced by the interpolated value. Removing these erroneous data points decreased the amount of variability in the high-frequency end of the computed power spectra.

The Fourier transform was computed with an algorithm described by Singleton (1967). This routine has the advantage that the number of points does not have to be a power of 2. After the spectrum was calculated it was smoothed by the function

$$P(i) = 1/64[P(i-3) + 6P(i-2) + 15P(i-1) + 20P(i) + 15P(i+1) + 6P(i+2) + P(i+3)]$$

as suggested by Endlich *et al.* (1969). The smoothing decreases the resolution but increases the statistical stability.

3. Frequency spectra and wind variability

The resulting spectra are shown in Fig. 2a and b. Fig. 2a represents the spectra for the zonal component at the five heights, and Fig. 2b shows the corresponding spectra for the meridional component. Spectra at successive heights have been multiplied by a factor of 100 to separate them on the graph. The units for the two spectra at 5.99 km altitude are correct. Least-squares fits of a function of the form

$$P(f) = P_0(f/f_0)^n$$

were made to determine the spectral index n. Here P is the power, and f is the frequency. The calculated value of n is shown next to the corresponding curve in Fig. 2a and b. A dashed line is used to show the fit. The least-squares computation was carried out for frequencies in the range from f = 0.015 h^{-1} to f = 0.45 h^{-1}. The average value of the spectral index for the zonal component is -1.604 ± 0.279. The average value of the index for the meridional component is -1.604 ± 0.259. The value of -1.604 is very close to $-5/3$. There is no particular reason to expect an $f^{-5/3}$ power law; however, if the Taylor transformation is valid in this range of frequencies, then a $k^{-5/3}$ power law is implied. This would correspond to an inertial subrange. There is no independent evidence from this study to indicate whether the Taylor transformation, i.e., that temporal scales are related to spatial scales by a constant factor of the mean

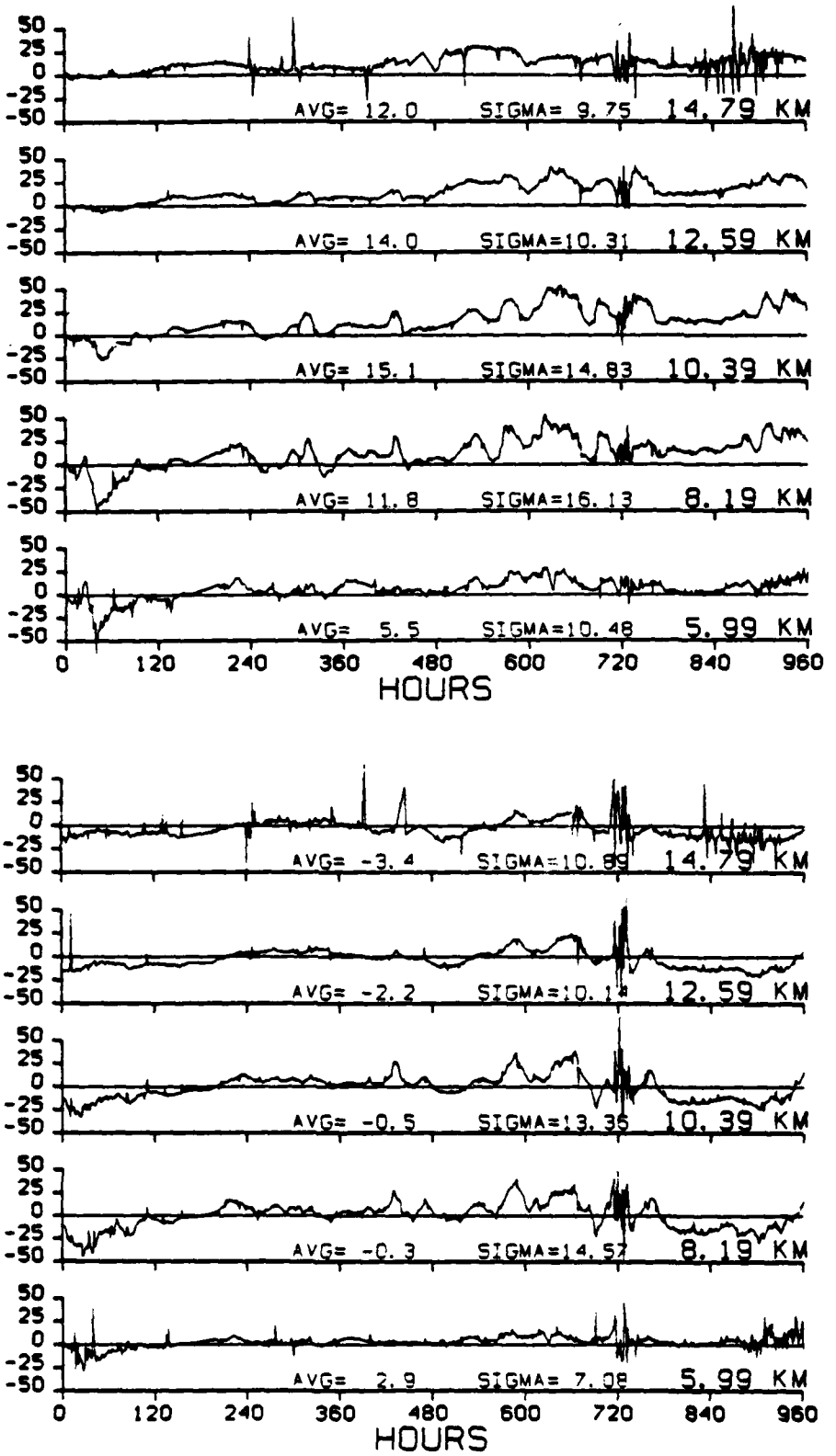

FIG. 1. The original data set of 960 hourly values at each of the five heights used in the study are shown as function of time. The average value and the variance at each of the heights are shown. The top half of the figure is for the zonal wind component, and the bottom half shows the meridional component.

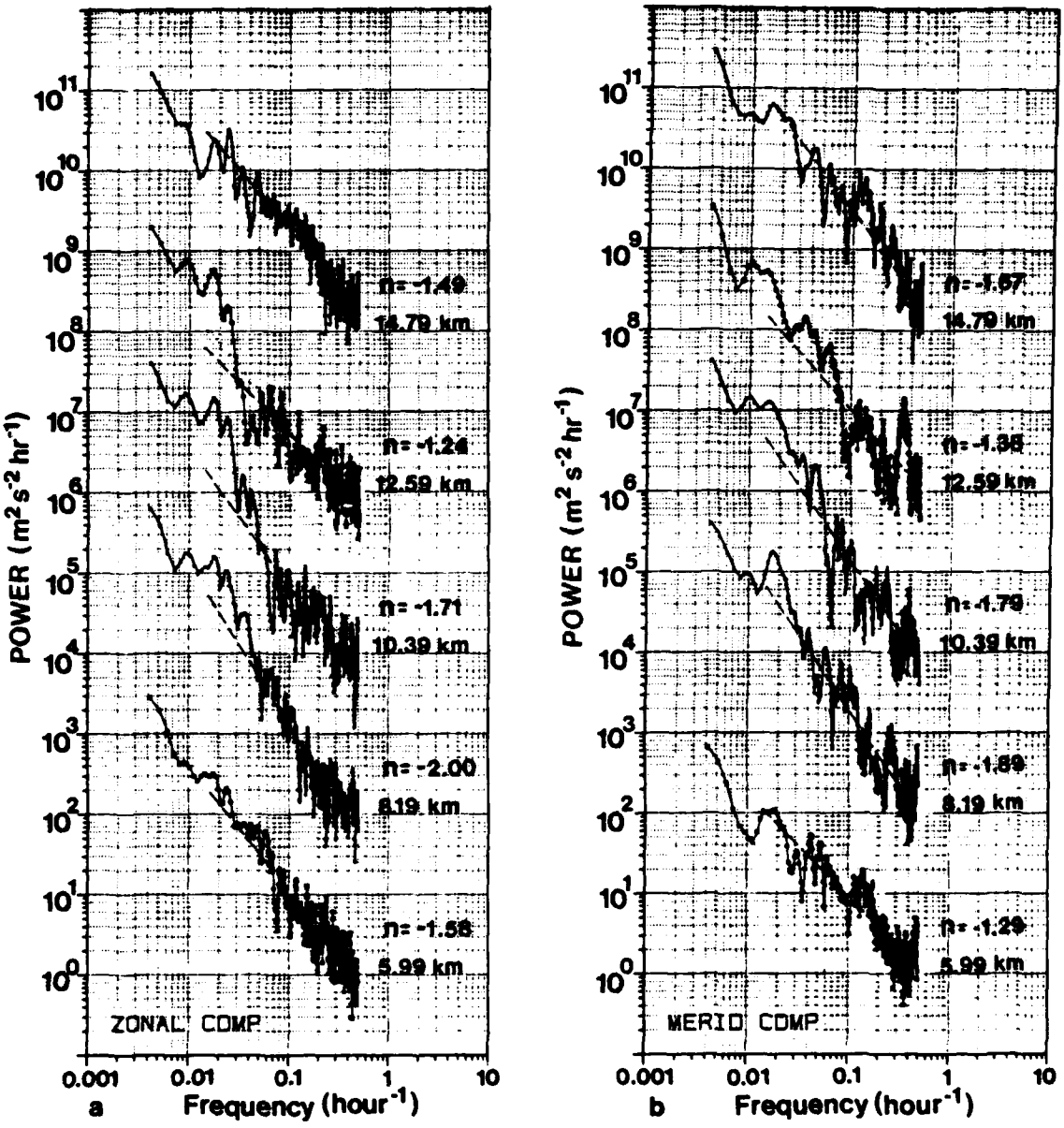

FIG. 2. (a) Power spectra for the time series of the zonal component shown in the previous figure. The parameter n at the right of each spectrum is the least-squares fit value of the spectral index. The average value of the spectral index is -1.604 ± 0.279. Spectra at successive heights have been multiplied by a factor of 100 to separate them on the graph. The axes are correct for the spectrum at 5.99 km. (b) The meridional wind component. The average value of the spectral index is -1.604 ± 0.259.

wind over the sampling time, is valid. However, the results of a study by Brown and Robinson (1979) in which European rawinsonde data were used indicated that the Taylor transformation can be used for spatial scales smaller than 1200 km and at least down to 200 km, the lower limit of the resolution of the network they used. The corresponding range of periods where the transformation was valid was in the range less than 2 days.

Gage (1979) summarized the diverse evidence for the existence of a $k^{-5/3}$ law inertial range at the meteorological mesoscale. He also used the variability calculated from a 7 h, high resolution, balloon wind measurement experiment and wind measurements made with the Sunset VHF Doppler radar in Colorado over a 14 h period to show that the lag variability defined by

$$\sigma_\tau = \overline{\{[v(t) - v(t+\tau)]^2\}}^{1/2}$$

follows a $\tau^{+1/3}$ power law out to time lags of at least 3–5 h. This is consistent with a $k^{-5/3}$ power law when

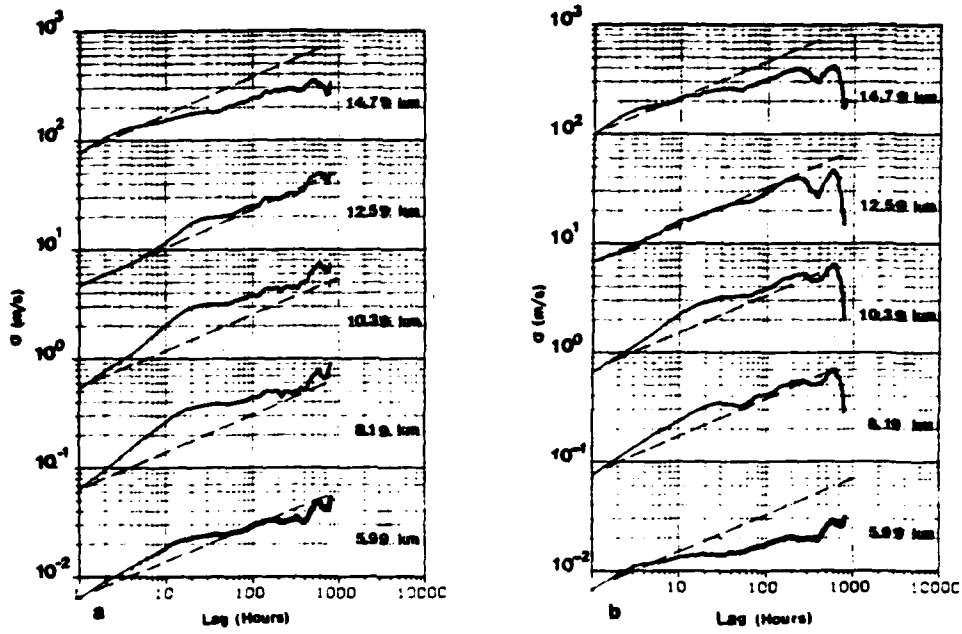

FIG. 3. (a) The variability of the zonal wind as a function of the time lag. The variability is defined in the text. Curves at successive altitudes have been multiplied by a factor of 10 to separate them on the graph. The vertical axis labeling is correct for the variance at 10.39-km altitude. (b) As in (a) but for the meridional wind component.

the Taylor transformation is valid as shown by Gage (1979).

Plots of the variability σ_r are presented in Fig. 3a and b for the zonal and meridional wind components respectively. Lines with a slope of $+\frac{1}{3}$ are superimposed on the curves for reference. Successive curves have been multiplied by a factor of ten to separate them on the graph. The scale is correct for the variance curve at 10.39 km altitude. Overall, the $\frac{1}{3}$ slope gives a reasonable fit to the curves. However, there is a pronounced "bump" with a peak near 25 h at 8.19, 10.39, and 12.59 km which is particularly noticeable in the zonal wind component. This peak in the variability should not be confused with a diurnal effect since a peak in the variability at 25 h, for instance, will correspond to a frequency with a period of 50 h. This can be seen in the spectra shown in Fig. 2a and b. A period of 50 h or 2.1 days would correspond to the wavenumber 3 Rossby-gravity mode discussed by Salby (1981) and seen with a number of other techniques summarized in that paper. The peak near 50 h in Fig. 2a corresponds to an amplitude of 1.4 m s^{-1}. The calculations of Salby (1981) show that the amplitude of the two-day wave decreases rapidly with increasing latitude. However, the amplitude is still 0.3 to 0.6 of the maximum zonal wind at the surface even at 65°N. An amplitude of 1.4 m s^{-1} gives a maximum surface wind of 4.67 m s^{-1} for the amplitude factor of 0.3. This is not unreasonable. A unique feature of the curves for the meridional wind is the rapid decrease in the variance for lags greater than 600 h or 25 days.

4. Discussion

In the preceding section it was shown that the frequency spectra for motions with periods in the range of 2 h out to ~50 h generally follow a $-\frac{5}{3}$ power law. This data set far exceeds any other published to date and complements the recent observations of Balsley and Carter (1982) who obtained spectra at 8 and 86 km also using the Poker Flat radar and Jasperson (1982) who determined lag variability for

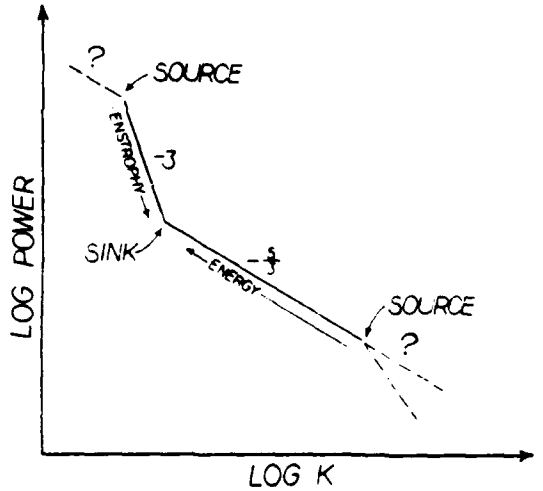

FIG. 4. Graph illustrating the wavenumber power laws that are discussed in the text. The direction of the flow of energy and enstrophy are shown together with the various sources and sinks.

sequential high-resolution wind profiles. Balsley and Carter found $-5/3$ law behavior extending over periods from a few minutes out to close to a day. From the results of 26 campaigns of high time-resolution, balloon wind-soundings, Jasperson found a $1/3$ power law for the lag variability for both components of the wind under anticyclonic conditions out to at least 4 h (the limit of his analysis). These observations taken together with the analysis of Brown and Robinson (1979) considerably strengthen the evidence for $-5/3$ power law behavior in the atmospheric mesoscale. As suggested by Gage (1979) this could be the result of a reverse energy cascading inertial range of two-dimensional turbulence.

Although the $-5/3$ law behavior seems indicative of a turbulence cascade process, others have advocated that mesoscale variability could alternatively be due to a spectrum of buoyancy waves (Dewan, 1979). Indeed, the existence of a spectrum of buoyancy waves is fairly well accepted in the ocean. This spectrum has been successfully modeled by Garrett and Munk (1972, 1975) and is often referred to as the Garrett-Munk spectrum. The Gararett-Munk spectrum has a universal character, and Van Zandt (1982) has recently shown that the same kind of approach can be applied to the atmosphere as well.

Lilly (1982) has recently considered the contributions of waves and turbulence to the mesoscale variability in the atmosphere. Extending the analysis of Riley *et al.* (1981) for wake collapse Lilly demonstrates that for low Froude number ($\equiv V'/NH$, where N is Brunt-Väisälä frequency, V' is the turbulence intensity, and H is a vertical scale) the equations of motion effectively decouple into a set of equations governing wave dynamics and another set of equations governing two-dimensional turbulence. Thus, according to Lilly, if the waves are free to propagate away from their region of generation, what remains is a field of two-dimensional turbulence. Lilly argues that the mesoscale atmospheric spectrum can be explained by an upscale energy cascading ("red" cascade) two-dimensional turbulence if as little as 1% of the small-scale forced turbulence participates in the red cascade. The remainder of the forced turbulence is dissipated in the usual way through a "blue" cascade associated with three-dimensional turbulence. Mechanisms which can force turbulence include convection, breaking waves and shearing instabilities. Once set in motion the red cascade presumably transfers energy to larger scales until it encounters the enstrophy cascade of geostrophic turbulence. The transition scale between the two regimes of two-dimensional turbulence should be $\sim$1000 km in the atmosphere. This is shown schematically in Fig. 4.

5. Conclusion

The Poker Flat MST radar has provided a high time resolution series of horizontal winds over a 40-day period. Spectral analysis of these winds reveals a $-5/3$ law behavior. This result adds to the accumulating evidence in favor of $-5/3$ law behavior throughout the atmospheric mesoscale. It also supports the idea of a reverse (energy) cascading two-dimensional inertial subrange in which energy is cascaded from small to large scales (Kraichnan, 1967; Gage, 1979; Lilly, 1982). The up-scale cascade presumably halts when the enstrophy cascading range of geostrophic turbulence (Kraichnan, 1967; Charney, 1971) is encountered at a scale of $\sim$1000 km. An alternative explanation for the observed mesoscale variability is a spectrum of buoyancy waves (Dewan, 1979; Van Zandt, 1982). In this connection Lilly (1982) has recently shown that waves can be expected to coexist with two-dimensional turbulence. A task for the future will be to determine how waves and turbulence combine to produce the observed spectra.

Acknowledgments. We are indebted to B. B. Balsley, D. Carter and W. Ecklund for all their work in obtaining the data, their helpfulness in furnishing it to us, and their willingness to discuss various aspects of it with us. We also thank T. Riddle for his efforts in generating the actual data tapes that we used. This research was supported by Grant AFOSR-80-0020.

REFERENCES

Balsley, B. B., and D. A. Carter, 1982: The spectrum of atmospheric velocity fluctuations at 8 mm and 86 mm. *Geophys. Res. Lett.* (in press).

——, and K. S. Gage, 1980: The MST radar technique: Potential for middle atmospheric studies, *Pure Appl. Geophys.*, **118**, 452-493.

——, W. L. Ecklund, D. A. Carter and P. E. Johnston, 1980: The MST radar at Poker Flat, Alaska. *Radio Sci.*, **15**, 213-224.

Beer, T., 1974: *Atmospheric Waves*. Wiley, 300 pp.

Brown, P. S., Jr., and G. D. Robinson, 1979: The variance spectrum of tropospheric winds over Eastern Europe. *J. Atmos. Sci.*, **36**, 270-286.

Cadet, D., 1978: The superpressure balloon sounding technique for the study of atmospheric meso- and microscale phenomena. *Bull. Amer. Meteor. Soc.*, **59**, 1119-1127.

Carter, D. A., B. B. Balsley and W. L. Ecklund, 1980: The Poker Flat MST radar: Signal analysis and data processing techniques with examples. *Preprints 19th Conf. on Radar Meteorology*, Miami, Amer. Meteor. Soc., 563-567.

Charney, J. G., 1971: Geostrophic turbulence. *J. Atmos. Sci.*, **28**, 1087-1095.

Chernikov, A. A., Y. V. Mel'nichuk, N. Z. Pinus, S. M. Shmeter and N. K. Vinnichenko, 1969: Investigations of the turbulence in a convective atmosphere using radar and aircraft. *Radio Sci.*, **4**, 1257-1259.

Desbois, M., 1975: Large-scale kinetic energy spectra from Eulerian analysis of Eole wind data. *J. Atmos. Sci.*, **32**, 1838-1847.

Dewan, E. M., 1979: Stratospheric wave spectra resembling turbulence. *Science*, **204**, 832.

Endlich, R. M., R. C. Singleton and J. W. Kaufman, 1969: Spectral analysis of detailed vertical wind speed profiles. *J. Atmos. Sci.*, **26**, 1030-1041.

——, and B. B. Balsley, 1978: Doppler radar probing of the clear atmosphere. *Bull. Amer. Meteor. Soc.*, **59**, 1074-1093.

Gage, K. S., 1979: Evidence for a $k^{-5/3}$ law inertial range in mesoscale two-dimensional turbulence. *J. Atmos. Sci.*, **36**, 1950–1954.

Garrett, C., and W. H. Munk, 1972: Space-time scales of internal wares. *Geophys. Fluid Dyn.*, **3**, 225–264.

——, and ——, 1975: Space-time scales of internal wares: A progress report. *J. Geophys. Res.*, **80**, 291–297.

Jasperson, W. H., 1982: Mesoscale time and space wind variability. *J. Appl. Meteor.*, **14**, (in press).

Julian, P. R., W. M. Washington, L. Hembree and C. Ridley, 1970: On the spectral distribution of large-scale atmospheric kinetic energy. *J. Atmos. Sci.*, **27**, 376–387.

Kao, S.-K., and H. N. Lee, 1977: The non-linear interactions and maintenance of the large-scale moving waves in the atmosphere. *J. Atmos. Sci.*, **34**, 471–485.

Kao, S.-K., and L. L. Wendell, 1970: The kinetic energy of the large-scale atmospheric motion in wavenumber-frequency space, I. Northern Hemisphere. *J. Atmos. Sci.*, **27**, 359–375.

Kao, S.-K., and H. D. Woods, 1964: Energy spectra of mesoscale turbulence along and across the jet stream. *J. Atmos. Sci.*, **21**, 513–519.

Kraichnan, R. H., 1967: Inertial ranges in two-dimensional turbulence. *Phys. Fluids*, **10**, 1417–1423.

Leith, C. E., and R. H. Kraichnan, 1972: Predictability of turbulent flows. *J. Atmos. Sci.*, **29**, 1041–1058.

Lilly, D. K., 1982: Stratified turbulence and the mesoscale variability of the atmosphere. Submitted to *J. Atmos. Sci.*

Lorenz, E. N., 1969: The predictability of a flow which possesses many scales of motion. *Tellus*, **21**, 289–307.

Mantis, H. T., 1963: The structure of winds of the upper troposphere at mesoscale. *J. Atmos. Sci.*, **20**, 94–106.

Riley, J. J., R. W. Metcalfe and M. A. Weissman, 1981: Direct numerical simulations of homogeneous turbulence in density-stratified fluids. Presented at the Workshop on Nonlinear Properties of Internal Waves, The LaJolla Institute, ONR, Physical Dynamics, 15–17 January, 60 pp.

Salby, M. L., 1981: The 2-day wave in the middle atmosphere: Observations and theory. *J. Geophys. Res.*, **86**, 9654–9660.

Singleton, R. C., 1967: On computing the fast Fourier transform, *Commun.* ACM, **10**, 647–654.

Van Zandt, T. E., 1982: A universal spectrum of buoyancy waves in the atmosphere. *Geophys. Res. Lett.* (in press).

Wooldridge, G., and E. R. Reiter, 1970: Large-scale atmospheric circulation characteristics as evident from GHOST balloon data. *J. Atmos. Sci.*, **27**, 183–194.

APPENDIX II

CAN A VHF DOPPLER RADAR PROVIDE SYNOPTIC WIND DATA?: A COMPARISON OF 30 DAYS OF RADAR AND RADIOSONDE DATA

Miguel Folkmar Larsen

School of Electrical Engineering

Cornell University

Ithaca, NY 14850

September 1981

Submitted to Mon. Wea. Rev.

Abstract. A number of experiments have shown that UHF and VHF Doppler radars can make clear air wind measurements in the troposphere and lower stratosphere. Past comparisons of radar and rawinsonde profiles for a single day have shown good agreement between the two within the limitations imposed by the spatial separation between the two measurements. However, the accuracy of the measurement does not insure that the data are synoptically significant. A comparison of 40 days of radiosonde geopotential height and wind data and radar data from Alaska was carried out to determine the applicability of the radar data to synoptic meteorology.

Rawinsonde and radar wind time series at a number of different heights were compared and the r.m.s. differences calculated. The two independent wind measurements were also compared to the geostrophic wind obtained from the geopotential height fields generated by applying the Cressman objective analysis scheme to data from five radiosonde stations surrounding the radar site. The two different wind measurements were most nearly similar with a difference of 3 to 4 m/s. The radar and balloon winds both differed from the geostrophic winds by 5 to 6 m/s. The r.m.s. errors decreased as the time over which the radar winds were averaged was increased. The cross-correlation between the measured and geostrophic winds was found to approximately 0.75 and essentially independent of height over the altitude range studied.

1. Introduction

The number of sensitive VHF and UHF Doppler radars being used for atmospheric research has increased considerably since the first measurements made by Woodman and Guillen (1974). Radars operating at wavelengths from 10's

of centimeters to several meters measure the winds from the Doppler shift of the signal backscattered from turbulent variations in the refractive index. Typical height and time resolutions are of the order of 100's of meters and several minutes. The technique and some of the early results have been reviewed by Gage and Balsley (1978), Rottger (1980), and Harper and Gordon (1980).

The first research applications of the long-wavelength radars were in the area of microscale dynamics, including turbulence in the troposphere and lower stratosphere and wave dynamics at scale sizes typical of gravity waves. Over the past few years there has been increasing interest in using the radar measurements for synoptic research and as part of the standard observational network. Larsen and Rottger (1982) have reviewed research applications, and Balsley and Gage (1982) have discussed some of the considerations involved in establishing an operational observing system. Carlson and Sundararaman (1982) have made strong arguments for the economic feasibility of implementing such a network. One of the most ambitious projects utilizing the radar technique operationally is part of the PROFS (Prototype Regional Observing and Forecasting System) program designed to improve mesoscale forecasting over periods of a day or less. PROFS includes a network of three VHF radars located in a triangle centered at Boulder, CO. Radar wind profiles are routinely processed and transmitted to the forecasting office once an hour (Hogg et al., 1980; Strauch, 1981; Strauch et al., 1982).

The relatively low cost of establishing a facility is part of the appeal of the radar systems. Also, very little maintenance or other manual

intervention is required once the facility is in operation (see e.g., Balsley et al., 1980). The present study was undertaken in order to determine if a VHF radar system of the type that would most likely be used operationally can provide wind data that is synoptically meaningful. The radar provides a very accurate wind measurement, i.e., a very accurate measurement of the velocity of the turbulent scatterers across the beam. The attainable accuracy is much greater than what would be useful in practice. However, the precision of the measurement may actually contaminate the synoptic wind profile with high frequency noise, making the data unusable. Also, the VHF radars typically operate with large fixed dipole arrays that look within a few degrees of vertical. Thus scans of large horizontal areas to determine the wind representative of some area greater than a predetermined horizontal scale size are not possible. However, it may be that averaging high time-resolution wind profiles can provide a suitable filtering. The next sections will investigate the amount of averaging that is necessary.

Errico (1982) has stated, "The degree to which the atmosphere satisfies various balance conditions will likely remain unknown for a long time because the data quality needed for that purpose will likely remain poor." The radar data's accuracy is sufficient to test the various balance conditions, and in this paper the simplest one, namely the geostrophic approximation, will be tested. Geostrophy will be used as a test of the synoptic applicability of the data, but the extent to which this relationship is satisfied is also of interest from the point of view of the various objective analysis schemes that use the approximation to relate the prediction error covariances between the

geopotential height and the wind components (see e.g., Bengtsson et al., 1982; Schlatter, 1975).

2. Synoptic applicability

The general meaning of synoptic applicability is clear based on the discussion above, but a specific quantitative comparison was needed for this study. The problem is, in fact, closely related to the problems of data assimilation and objective analysis for numerical models (see e.g., Bengtsson et al., 1981). The latter attempts to treat a set of observations in such a way that high frequency waves that lead to numerical instabilities are eliminated. A balance condition of one kind or another is used to accomplish this, the simplest being a geostrophic balance (e.g., Cressman, 1959) and the most complicated being the balance derived from the model dynamics and termed normal mode initialization (e.g., Daley, 1981).

In this study I will compare radar wind data taken over a 30 day period from March 1 to April 1, 1979 and radiosonde data taken at the standard observational hours during the same period. The radar is located at Poker Flat, Alaska (see Balsley et al., 1980 for a description), and the nearest radiosonde station is at Fairbanks, 35 km southeast of the radar. The radar measures one complete wind profile every 4 min between the surface and 14.79 km, but these high time-resolution measurements are likely to be contaminated by high-frequency meteorological "noise." In order to test whether or not the radar can provide useful synoptic scale wind information, comparisons were made between the geostrophic wind derived by applying an objective analysis scheme to the geopotential height data from five surrounding radiosonde stations and

the radar winds averaged over various time intervals. Radar and rawinsonde winds were also compared.

A test of geostrophy is not the best test possible, but a simple, yet useful, comparison was needed for the purpose of this initial study. Also, the differences between the radar, rawinsonde, and geostrophic winds are of interest from the point of view of the multivariate objective analysis schemes that use geostrophy to relate height-height autocorrelations to the height-wind cross-correlations (e.g., Rutherford, 1973; Schlatter, 1975; Schlatter et al., 1976; Bergman, 1979; Lorenc, 1982). Finally, the radar wind measurements are the first independent measurements with accuracy and height resolution comparable to or better than the rawinsonde. The results of this study show that the radar and rawinsonde measurements are most similar in the r.m.s. (root mean square) sense, and both differ from the geostrophic wind by approximately the same amount.

I will describe the radar and radiosonde data sets in the next section. Radar and rawinsonde wind measurements are compared in the following section. Next, radar and rawinsonde measurements are compared to the geostrophic winds derived from the geopotential height data. The last section contains a general discussion of the implications of the results.

3. Description of the data sets

During the spring of 1979, the Poker Flat MST radar consisted of a 100 m x 100 m fixed dipole array. The antenna size has since been expanded to 200 m x 200 m. The horizontal wind vector was measured by two beams pointed 15°'s off vertical, one with an azimuth pointing close to north and one pointing

close to east. Corrections were applied to the data to get the exact zonal and meridional wind components. One complete wind profile was obtained every 4 min with a height resolution of 2.2 km. In the troposphere and lower stratosphere wind data was routinely available at six consecutive heights beginning at 3.79-km altitude. All altitudes for radar data referred to from here on are at the center of the range gate. The wind measurement is in some sense an average over 2.2 km weighted by the intensity of the turbulent layers in the volume illuminated by the radar beam. Sato and Fukao (1982) have pointed out that having a number of turbulent layers within the range gate can lead to errors in the measurement if there is a strong shear across the range gate. However, such an effect will not be considered further here.

The signal voltages measured by the receiver are Fourier Transformed to obtain the Doppler spectrum. The frequency spectrum measured by scattering from a turbulent process will be a Gaussian for a normal random process as discussed by Woodman and Guillen (1974) and others. The accuracy with which the velocity of the turbulent scatterers in the radar volume can be determined is only limited by the rate at which the signal is sampled and the accuracy with which the Gaussian can be fit to the spectrum. Accuracies better than 1 cm/s can be achieved in practice, but there is no need to measure the horizontal wind components that accurately. The error for the radar data discussed here is approximately 1 m/s. When all three wind components are measured simultaneously, the vertical beam is sampled at a higher rate than the off-vertical beams to attain the much higher accuracy needed for vertical velocity measurements.

The horizontal vector winds were derived from the off-vertical wind components with the assumption that the vertical velocity was negligible. In most cases such an assumption is justified as more recent data sets in which all three wind components were measured have shown (T. Riddle, Aeronomy Lab, NOAA, private communication, 1982). However, there are times when the vertical velocity can make a significant contribution over a period spanning several consecutive profiles. In order to minimize any such effect, the radar wind data was averaged over an hour. The time series of the hourly-average zonal and meridional wind components are plotted in Figure 1 taken from Larsen et al. (1982).

The radiosonde data provided by the National Climatic Center is from the five nearest National Weather Service (NWS) radiosonde stations as shown in Figure 2. Only launches at 00 GMT and 12 GMT are available for the period discussed here. No supplemental launches are included in the data set. The radiosonde station closest to Poker Flat is at Fairbanks, 35 km southeast of the radar site. Anchorage, McGrath, Barter Island, and Yakutat are 455 km, 476 km, 572 km, and 764 km from the radar site respectively.

The balloon wind data was interpolated linearly between the two nearest significant levels to the altitude corresponding to the center of each of the radar range gates. The interpolation was applied independently to the speed and the direction. The pressure at the seven different radar heights was determined from the Fairbanks radiosonde data. The formula for a hydrostatic atmosphere with a constant lapse rate was used to interpolate the pressure between the two nearest significant levels. The same formula was then applied

to the radiosonde data from the other four stations to find the height of the pressure surface intersecting the center of each of the radar range gates.

4. Comparison of radar and rawinsonde wind measurements

The rawinsonde and radar winds for the period from March 1 to April 1, 1979 are plotted in Figure 3 for seven consecutive heights. The heavy solid line is the rawinsonde measurement and the light dashed line is the radar measurement. The signal-to-noise ratio at 16.99 km is too low to derive a meaningful signal from the echoes, but the time series at this height has been plotted for reference nonetheless. The radar winds are 1-hour averages as mentioned previously while the rawinsonde data is from a single ascent. The root-mean-square (r.m.s.) difference between the two measurements is indicated by the quantity labeled "sigma".

The two curves follow each other very closely until day 78 but deviate significantly from each other after that. The r.m.s. differences range from a minimum of 3.21 m/s to a maximum of 9.30 m/s in the zonal component and from a minimum of 4.66 m/s to a maximum of 12.73 m/s in the meridional component. The variation of sigma with height follows the variation of the mean wind for the period as a function of height. The mean wind has been plotted in Figure 4. Schlatter (1975) also found that the difference between the objectively analyzed wind and the measured wind varied as the mean wind profile.

The differences in the winds measured at the two locations with the two different techniques can be attributed to a combination of three factors. First there are errors in the wind measurements. Second there is variability in the wind over the distance between the two sites. Third there is temporal

variability. The rawinsonde takes approximately 1 hour to ascend through the height range where reliable measurements can be made by the radar. The radar measurements presented here are 1-hour averages, but the rawinsonde will only spend a few minutes within any one of the radars range gates.

It should be possible to decrease the r.m.s. differences between the two wind measurements by averaging the measurements over longer time intervals if some of the difference is due to small-scale temporal and spatial variability and if the winds are statistically well behaved. Indeed, that is the case. Figure 5 shows the comparison between the 24-hour average rawinsonde and radar winds. The radar average consists of 24 hours of wind profiles taken every 4 minutes. The rawinsonde average consists of three wind profiles, one taken at either 00 or 12 GMT and the profile preceding and following it. The r.m.s. differences have decreased to a maximum of 6.52 m/s in the zonal component and a maximum of 7.33 in the meridional component.

Figure 6 shows a comparison of the 12-hour average radar winds and the winds measured by individual rawinsonde ascents. In other words, the averaging interval has been increased for the radar when compared to Figure 3 but not for the rawinsonde. The r.m.s. differences still decrease significantly when compared to the case of the 1-hour averages. The difference between Figures 3 and 6 is primarily that many of the large spikes in the radar data have been eliminated. The original time series shown in Figure 1 have quite a few large spikes. Some of them are isolated, but a number of them occur during periods of high variability indicating that they are likely to be real. Averaging decreases the large errors that arise due to this effect. The rawinsonde winds

do not exhibit any of these spikes in spite of the fact that they are not averaged over long time intervals as the radar winds are. However, the profiles are routinely edited to delete wind data at any heights characterized by large changes in wind direction or wind speed over 1 to 2 min intervals during the ascent. An attempt was made to subject the radar data to the same type of screening. The exact criteria could not be applied since 1 to 2 min of balloon ascent correspond to approximately 300 to 600 m. The height resolution of the radar measurements is 2.2 km. Thus, the rawinsonde criteria were linearly extrapolated by multiplying the change over 600 m by the appropriate factor to get the corresponding change over 2.2 km. There is little doubt that the two procedures are not equivalent. In any case, there was little difference between the results when the error criteria were and were not applied to the radar data.

Figures 3, 5, and 6 all show a similar behavior in one respect. The agreement between the radar and rawinsonde wind measurements is quite good until day 78. After that a large discrepancy arises. One would suspect that most of the r.m.s. difference between the two measurements is attributable to the period from day 78 til the end. I will show later that the statistics are quite different for the first half and the last half of the month and discuss possible reasons for such an effect.

5. Comparison of measured winds and geostrophic winds

The Cressman analysis is an objective analysis scheme used to interpolate data from irregularly spaced grid points to a regular grid suitable for analysis or input to a numerical model. Given a series of observations f_i'

where the index i ranges over the number of observations that influence the grid point, the value of f at the grid point f_g will be given by

$$f_g^i = f_g^x + \sum_{i=1}^{n} C_i^f f_i' \qquad (1)$$

The quantity f_g^c is an initial guess of the value of f at the grid point. The initial value will be modified by the observed changes from the initial guesses at the observation points given by $f_i' = f_i^o - f_i^c$. The actual observed value is f_i^o. The weighting function is given by $C_i f = 1/n \cdot (R^2 - D^2)/(R^2 + D^2)$ where R is the radius of influence and D is the distance from the observation point to the grid point. The weight is zero if D is greater than R. The distance D was calculated from the formula given by Schlatter (1975)

$$D = r_E\{(\phi_g - \phi_i)^2 \cos^2[1/2(\theta_g + \theta_i)] + (\theta_g - \theta_i)^2\}^{1/2} \qquad (2)$$

where r_E is the radius of the earth, θ is latitude, and ϕ is longitude. The form of the objective analysis scheme used here has been described in detail by Kruger (1969).

The geostrophic wind components were derived from the observed values of the geopotential height at the five radiosonde stations shown in Figure 2. Values were interpolated to a grid with a spacing of 100 km and aligned along the north-south and east-west axes. The central grid point was positioned to coincide with the location of the Poker Flat radar. Typically, the interpolation procedure would be confined to fixed pressure surfaces. However, the radar measures the velocity at a fixed height irrespective of pressure. Thus, the initial guesses of the geopotential height at the observation points

had to be derived in a slightly different way. The pressure at the height of the seven different radar ranges was calculated based on the Fairbanks sounding. The height of the corresponding pressure surface at the four surrounding radiosonde stations was calculated, and the derived height values at a given station were then averaged for the entire 40 day period during which data was available. Therefore, the initial or climatological value of the height at a given radiosonde station is the average geopotential height, for the period, of the average pressure surface corresponding to the height of the radar range gate at Poker Flat.

The 24-hour average radar winds are plotted in Figure 7 together with the geostrophic wind calculated from the height field obtained by applying the procedure described above. The r.m.s. differences are larger than those between the radar and rawinsonde wind measurements. Also, the errors are much larger in the meridional component than in the zonal component. It appears that most of the contribution to the large r.m.s. differences come from the second half of the time series. Figure 8 is similar to Figure 7 but shows the 24-hour average rawinsonde winds as opposed to the 24-hour average radar winds. The r.m.s. differences between the two wind measurements and the geostrophic winds are comparable, but that is not surprising since it was noted in the last section that the two wind measurements are very similar.

The behavior of the differences between the radar winds and the geostrophic winds is summarized in Figures 9a and 9b. The error decreases as the averaging interval is increased in both the zonal and meridional component. Although, the error decreases significantly when the averaging interval is

increased from 1 hour to 12 hours, particularly in the meridional component, the reduction is relatively small when the averaging interval is increased further. The error is much larger in the meridional component than in the zonal component. The overall shape of the curves is very similar to the shape of the mean wind profile shown in Figure 4.

The r.m.s. differences between the three 24-hour averages are shown in Figures 10a for the zonal component and 10b for the meridional component. There is very little difference between the three for the zonal component, although the radar and balloon wind measurements are most similar at the two highest altitudes. The radar and balloon winds are most similar for the meridional component except at the two lowest altitudes. It appears that in general the differences between the two independent wind measurements are smaller than the differences between the measured and geostrophic winds, but the changes are so small that it is difficult to justify any inferences on the basis of these results. However, when the first and second half of the data sets are treated separately, the relationship is much clearer.

6. Comparison of first and second half of data set

A close examination of Figures 3, 5, 6, 7, and 8 shows that most of the contribution to the r.m.s. differences between the radar and rawinsonde winds, the radar winds and the geostrophic wind, and the rawinsonde winds and the geostrophic winds derives from the time period between day 78 and day 92, the end of the period when data is available. The time series were divided into two segments, one from March 1 to March 16 and the other from March 17 to April 1. The r.m.s. differences were calculated for each half for 1-hour and 24-hour

averages. The large deviations occur later than March 17, but the data set was divided in half so as not to change the statistics simply due to differences in the number of samples in each set.

Table I shows that all errors are comparable in the second half of the data set for both the 1-hour and 24-hour averages. However, the relationships that emerged when the time period was treated as a whole are much clearer in the first half. When a 1-hour average of the radar data is compared to a single rawinsonde ascent, the differences are 3.19 m/s in the zonal component and 4.03 m/s in the meridional component. The differences between the radar and geostrophic winds, and the rawinsonde and geostrophic winds are nearly identical and 1.5 to 2.0 m/s greater than the difference between the radar and rawinsonde winds. Averaging for 24 hours decreases the difference between the two independent wind measurements to 2.21 m/s and 3.10 m/s. The difference between the measured winds and the geostrophic winds is still 1.5 to 2.0 m/s greater than the difference between the two wind measurements.

7. Effect of varying the radius of influence

All of the curves so far have shown results for a Cressman objective analysis scheme with a radius of influence of 750 km. This particular radius was chosen because it was the optimum value when the entire height range where radar data was available was considered. Figures 11a and 11b show the r.m.s. differences between the 24-hour average radar winds and the geostrophic winds as a function of the radius of influence. The 750 km value gives the best result over all, although at the two lowest altitudes the best result is achieved when R=1000 km. However, the difference in the errors when the larger

value is used is very small below the tropopause but can amount to 1 to 2 m/s at the tropopause and in the lower stratosphere. A radius of influence of 750 km also gives the best result for the meridional component, but the error is much less dependent on the radius chosen in this component than in the zonal component.

The Gandin objective analysis scheme described by Kruger (1969) was also tested. The basic difference is in the weighting function. While the Cressman analysis uses a parabolic weighting function, the Gandin method uses a Gaussian weighting, and both schemes are univariate. I will not present the results in graphic form since the difference in all cases was only a fraction of a m/s, less than the accuracy of the radar measurements during the spring of 1979.

The Cressman analysis is often applied in a series of successive scans (Cressman, 1959; Otto-Bliesner et al., 1979). A large radius of influence is chosen initially so as to include information from many stations surrounding the grid point. The radius is then decreased successively, until finally only the nearest stations affect the analyzed value. The successive scans method was also applied to the Alaska radiosonde data. The initial radius was 2000 km, and it was decreased by 400 km in each of four successive passes through the data. The result of this analysis was actually worse than the single scan with a radius of 750 km. The average difference in the r.m.s. error was slightly greater than 1 m/s. The successive scans method produced more variability in the geostrophic winds calculated from the analyzed geopotential height fields, but the short term variations did not improve the agreement with the radar or rawinsonde winds.

8. Correlation between winds and geopotential heights

The correlation coefficients between the zonal winds and geopotential heights are plotted in Figure 12. Multivariate objective analysis schemes such as those of Schlatter (1975), Rutherford (1973), and Bergman (1979) carry out the objective analysis procedure based on both height and wind data. The wind information supplements the observed height field data when the two quantities are related through the geostrophic relation. The procedure in effect assumes that the correlation between the height fields and the winds is unity at zero spatial separation. Figure 12 shows the correlation coefficient for a 24-hour average wind to be nearly independent of height with a value of approximately 0.75.

Since the statistics for the r.m.s. differences were clearly very different for the first and second half of the data sets, the correlation coefficients were also calculated separately for each half. The results are shown in Table II. The correlations are nearly identical in both halves unlike the situation for the r.m.s. differences. When the averaging interval is increased from 1 hour to 24 hours, the correlations increase for both the radar/rawinsonde comparison and the radar/geostrophic wind comparison. The same is not true for the rawinsonde/geostrophic wind comparison. The correlation coefficients are virtually identical for the 1-hour average, i.e., single profile, and 24-hour average, i.e., three-profile, comparisons. Again, the filtering applied to the height variations in the balloon wind measurements is a possible explanation for this result.

9. Comparison with earlier results

Most previous estimates of the synoptic error of the rawinsonde wind measurements have involved comparisons of observed values and the output grid values from numerical models or objective analysis procedures (e.g., Lyne et al., 1982; Bergman, 1979; Bengtsson et al., 1982). Such an approach was necessitated by the lack of another measurement technique with accuracy comparable to the rawinsonde measurement as shown in the article by Bengtsson et al. (1982) where a summary of the estimated accuracies of the various wind measurements used operationally is presented. Also, the comparison between observations and model or objective analysis output is of direct interest since it provides a direct estimate of the magnitude of the unbalanced wind component in the observation.

Lyne et al. (1982) found the error to be between 3 m/s at low levels and 4 m/s and high levels near 100 mb. Their results are roughly consistent with, though smaller than, the range of 2 to 6 m/s given by Bengtsson et al. (1982). Both sets of errors are much smaller than the best case estimate of 7.98 m/s at 500 mb calculated by Bergman (1979). However, the latter was based on assumed values for the magnitude of the errors that are needed for the optimum interpolation objective analysis scheme. The errors found in this study by direct comparison of the balloon and radar measurements were 3.19 m/s for the zonal component and 4.03 m/s for the meridional component, in good agreement with the results of Lyne et al. (1982). Since there is a 35-km separation between the radar facility and the rawinsonde station, there is an error component due to small-scale spatial variations. However, the 4-min radar data were averaged for an hour in order to reduce such effects. The r.m.s.

difference between the two wind measurements decreased by approximately 1 m/s when the averaging interval was increased to 24 hours.

The high-time resolution wind measurements and the comparison with the balloon data has made it possible to obtain an estimate of the magnitude of the ageostrophic wind component based directly on measurements. Although the difference between the radar and balloon wind measurements decreased as the averaging interval increased, the difference between the measured wind and the geostrophic wind remained constant at approximately 2 m/s (Table I shows the exact values).

Table I shows that there is a clear difference between the first half of the period studied and the second half. In the first half, the two wind measurements are very similar and the estimate of the ageostrophic wind component is the same based on both techniques. In the second half, the differences between the radar and balloon wind measurements are much larger than in the first half, and the difference between the measured and geostrophic winds is about the same as the difference between the two independent wind measurements. The data processing for the radar data did not change in any way during the month, and none of the radar components such as transmitters or receivers were modified or failed during this period. Thus, there is no reason to expect a deterioration in the quality of the radar data. Also, the comparisons involving the balloon measurements are as poor at this time as those involving the radar. I have examined the 500-mb charts for the entire period, but there was no fundamental differences in the overall flow pattern during the first and second half of the month. One difference that is evident

in Figure 1 is the amount of short term variability in the radar data after the time labeled 600 hours. Aside from the episode of very large and rapid variations at 720 hours, there is consistently more variability overall. Table III shows the variance of the radar winds at each height for the first and second half of the period and supports this conclusion. Warner Ecklund (Aeronomy Lab, NOAA, private communication, 1982) has indicated that a major difference between summer and winter data both at Poker Flat, Alaska and Platteville, Colorado is in the amount of power in small time-scale variability, although he was not aware of any sharp transitions such as the one noted here. Whether this is indeed a summer/winter transition effect will have to be investigated further.

10. Conclusion

This study has shown that a VHF radar operated continuously in a mode such as the Poker Flat MST radar can provide synoptically meaningful data. Comparison of the radar wind measurements and radiosonde pressure and wind data has made it possible to assess the accuracy of the rawinsonde directly and to estimate the magnitude of the ageostrophic wind component. The balloon wind measurement error was found to be comparable to errors found by Lyne et al. (1982) using a primitive equation numerical model and four-dimensional data assimilation during the FGGE experiment. As the averaging interval was increased, the error decreased further.

If the radar data is used in the future for synoptic applications, the data will either have to be averaged temporally over some period appropriate to the numerical model that is used or a vertical variation filter such as that

applied to the rawinsonde data will have to applied. The results of this study will help in designing criteria for the former case. The latter case could not be investigated using the Poker Flat data that is presently available since the height resolution is too coarse to apply the empirical rawinsonde filters.

The data set studied here was the first long time series of horizontal winds produced by the Poker Flat radar. Beginning in the early part of 1981, the radar was operated continuously and measured all three wind components simultaneously. The longer data set should be used to check the preliminary results presented here, including the possibility of a seasonal variation in the short term variability. Finally, the same types of comparisons should be carried out with some of the better objective analysis schemes that are now available. In particular, the normal mode method has many advantages in that it not only produces analyzed fields that are exactly consistent with a given numerical model, but it can also be used to determine the contributions from the fast (gravity wave) and slow (inertio-gravity and Rossby wave) components separately.

The radar measurements have been shown to produce data of a quality that is at least comparable to the earlier estimates of accuracy of the rawinsonde when the radar data is averaged for an hour or more. Of course, that is not the limit of the usefulness of the radar data since it can routinely provide 1-hour or even higher time resolution data. Such a capability will become increasingly useful as the smallest scales resolved by numerical models decreases further.

Acknowledgments. I am grateful to Ben B. Balsley, Dave Carter, and Warner

Ecklund of the Aeronomy Lab at NOAA for many useful discussions concerning the radar data, and particularly to Tony Riddle for generating data tapes in a convenient format and for answering many questions about the data processing. This research was sponsored by the Air Force Office of Scientific Research under grant AFOSR-80-0020.

References

Balsley, B.B., W.L. Ecklund, D.A. Carter, and P.E. Johnston, 1980: The MST radar in Poker Flat, Alaska. Radio Sci., 15, 213-224.

Balsley, B.B., and K.S. Gage, 1982: On the use of radars for operational wind profiling. Bull. Amer. Meteorol. Soc., 63, 1009-1018.

Bengtsson, L., M. Ghil, and E. Kallen (eds.), 1981: Dynamic Meteorology: Data Assimilation Methods, Applied Mathematical Sciences Series, Vol. 36, Springer-Verlag, New York, 330 pp.

Bengtsson, L., M. Kanamitsu, P. Kallberg, and S. Uppala, 1982: FGGE 4-dimensional data assimilation at ECMWF. Bull. Amer. Meteorol. Soc., 63, 29-43.

Bergman, K.H., 1979: Multivariate analysis of temperature and winds using optimum interpolation. Mon. Wea. Rev., 107, 1423-1444.

Carlson, H.C., Jr. and N. Sundararaman, 1982: Real-time jetstream tracking: National benefit from an ST radar network for measuring atmospheric motions. Bull. Amer. Meteorol. Soc., 63, 1019-1026.

Cressman, G.P., 1959: An operational objective analysis system. Mon. Wea. Rev., 87, 367-374.

Daley, R., 1981: Normal mode initialization. Rev. Geophys. Space Phys., 19,

450-468.

Errico, R.M., 1982: Normal mode initialization and the generation of gravity waves by quasi-geostrophic forcing. J. Atmos. Sci., 39, 573-586.

Gage, K.S., and B.B. Balsley, 1978: Doppler radar probing of the clear atmosphere. Bull. Am. Meteorol. Soc., 59, 1074-1093.

Harper, R.M., and W.E. Gordon, 1980: A review of radar studies of the middle atmosphere. Radio Sci., 15, 195-211.

Hogg, D.C., F.O. Guiraud, C.G. Little, R.G. Strauch, M.T. Decker, and E.R. Westwater, 1980: Design of a ground-based remote sensing system using radio wavelengths to profile lower atmospheric winds, temperature, and humidity. In Remote Sensing of Atmospheres and Oceans, Academic Press, New York, pp. 313-364.

Kruger, H.B., 1969: General and special approaches to the problem of objective analysis of meteorological variables. Quart. J. Roy. Meteorol. Soc., 95, 21-39.

Larsen, M.F., M.C. Kelley, and K.S. Gage, 1982: Turbulence spectra in the upper troposphere and lower stratosphere at periods between 2 hours and 40 days. J. Atmos. Sci., 39, 1035-1041.

Larsen, M.F., and J. Rottger, 1982: VHF and UHF Doppler radars as tools for synoptic research. Bull. Amer. Meteorol. Soc., 63, 996-1008.

Lyne, W.H., R. Swinbank, and N.T. Birch, 1982: A data assimilation experiment and the global circulation during the FGGE special observing periods. Quart. J. Roy. Meteorol. Soc., 108, 575-594.

Otto-Bliesner, B., D.P. Baumhefner, T.W. Schlatter, TTd R. Bleck, 1977: A

comparison of several meteorological analysis schemes over a data-rich region. Mon. Wea. Rev., 105, 1083-1091.

Rottger, J., 1980: Structure and dynamics of the stratosphere and mesosphere revealed by VHF radar investigations. Pure Appl. Geophys., 118, 494-527.

Rutherford, I.D., 1972: Data assimilation by statistical interpolation of forecast error fields. J. Atmos. Sci., 29, 809-815.

Sato, T. and S. Fukao, 1982: Altitude smearing due to instrumental resolution in MST radar measurements. Geophys. Res. Lett., 9, 72-75.

Schlatter, T.W., 1975: Some experiments with a multivariate statistical objective analysis scheme. Mon. Wea. Rev., 103, 246-257.

Strauch, R.G., 1981: Radar measurement of tropospheric wind profiles. Preprints, 20th Conference on Radar Meteorology (Boston), AMS, Boston, pp. 430-434.

Strauch, R.G., M.T. Decker, and D.C. Hogg, 1982: An automatic profiler of the troposphere. Preprints, AIAA 20th Aerospace Sciences Meeting (Orlando, Fla.), American Institute of Aeronautics and Astronautics, New York.

Williamson, D.L., R.G. Daley, and T.W. Schlatter, 1981: The balance between mass and wind fields resulting from multivariate optimal interpolation. Mon. Wea. Rev., 109, 2357-2376.

Woodman, R.F., and A. Guillen, 1974: Radar observations of winds and turbulence in the stratosphere and mesosphere. J. Atmos. Sci., 31, 493-505.

Figure Captions

Figure 1. Original data set of 30 days of hourly values measured by the Poker Flat, Alaska MST radar beginning on March 1 and ending on April 1, 1979. The top half of the figure is for the zonal wind and the bottom half is for the meridional wind component.

Figure 2. Map showing the location of the five radiosonde stations closest to the site of the Poker Flat radar.

Figure 3. Comparison of 1-hour average radar winds (light dashed line) and rawinsonde wind measurements (heavy solid line) at seven successive heights during March 1979. The r.m.s. (root-mean-square) differences are shown at bottom right-hand-side of each box.

Figure 4. Mean wind profile for the 30 day period based on the radar wind measurements. The zonal and meridional wind components were averaged separately to determine the curves.

Figure 5. Comparison of 24-hour average radar winds (light dashed line) and averages of three successive rawinsonde wind measurements (heavy solid line).

Figure 6. Comparison of 12-hour average radar winds (light dashed line) and single rawinsonde measurements (heavy solid line).

Figure 7. Comparison of 24-hour average radar winds (light dashed line) and the geostrophic wind (heavy solid line). The geostrophic wind was calculated from a grid of geopotential height values derived using the Cressman objective analysis scheme with a radius of influence of 750 km.

Figure 8. Same as Figure 7 but for an average of three successive rawinsonde measurements instead of the radar wind measurements.

Figure 9a. Summary plot of the r.m.s. differences beween the zonal component of the radar winds and geostrophic winds for various averaging intervals.

Figure 9b. Same as Figure 9a but for the meridional wind component.

Figure 10a. Summary plot of the r.m.s. differences for the radar/geostrophic wind, radar/rawinsonde, and rawinsonde/geostrophic wind comparisons for the zonal component.

Figure 10b. Same as Figure 10a but for the meridional wind component.

Figure 11a. Differences between the 24-hour average radar winds and the geostrophic winds for various radii of influence for the zonal wind component.

Figure 11b. Same as Figure 11a but for the meridional component.

Figure 12. Cross-correlation between the 24-hour average radar and geostrophic winds, between the radar and rawinsonde winds, and between averages of three successive rawinsonde measurements and the geostrophic winds. The correlations are for the zonal wind component. Values for the meridional component are similar.

1-HOUR AVERAGES

	3/1/79-3/16/79		3/17/79-4/1/79	
	u	v	u	v
Radar vs. Rawinsonde	3.19	4.03	8.45	10.70
Radar vs. Cressman Analysis	5.67	5.57	8.40	12.37
Rawinsonde vs. Cressman Analysis	6.54	5.30	6.08	8.84

24-HOUR AVERAGES

	3/1/79-3/16/79		3/17/79-4/1/79	
	u	v	u	v
Radar vs. Rawinsonde	2.21	3.10	5.59	6.44
Radar vs. Cressman Analysis	4.66	4.60	5.79	8.95
Rawinsonde vs. Cressman Analysis	5.29	4.60	5.20	8.22

Table 1

1-HOUR AVERAGES

	3/1/79-3/16/79		3/17/79-4/1/79	
	u	v	u	v
Radar vs. Rawinsonde	0.541	0.529	0.522	0.550
Radar vs. Cressman Analysis	0.589	0.470	0.545	0.504
Rawinsonde vs. Cressman Analysis	0.661	0.734	0.676	0.829

24-HOUR AVERAGES

	3/1/79-3/16/79		3/17/79-4/1/79	
	u	v	u	v
Radar vs. Rawinsonde	0.768	0.712	0.702	0.834
Radar vs. Cressman Analysis	0.700	0.503	0.682	0.685
Rawinsonde vs. Cressman Analysis	0.691	0.731	0.712	0.826

Table 2

VARIANCES OF RADAR WINDS

	3/1/79-3/16/79		3/17/79-4/1/79	
	U	V	U	V
3.79 KM	4.40	2.49	5.89	8.24
5.99 KM	4.88	2.89	7.44	6.36
8.19 KM	8.67	6.10	11.39	16.72
10.39 KM	6.63	6.15	11.51	16.40
12.59 KM	5.14	5.75	8.39	13.04
14.79 KM	7.96	9.79	10.05	12.78

TABLE III

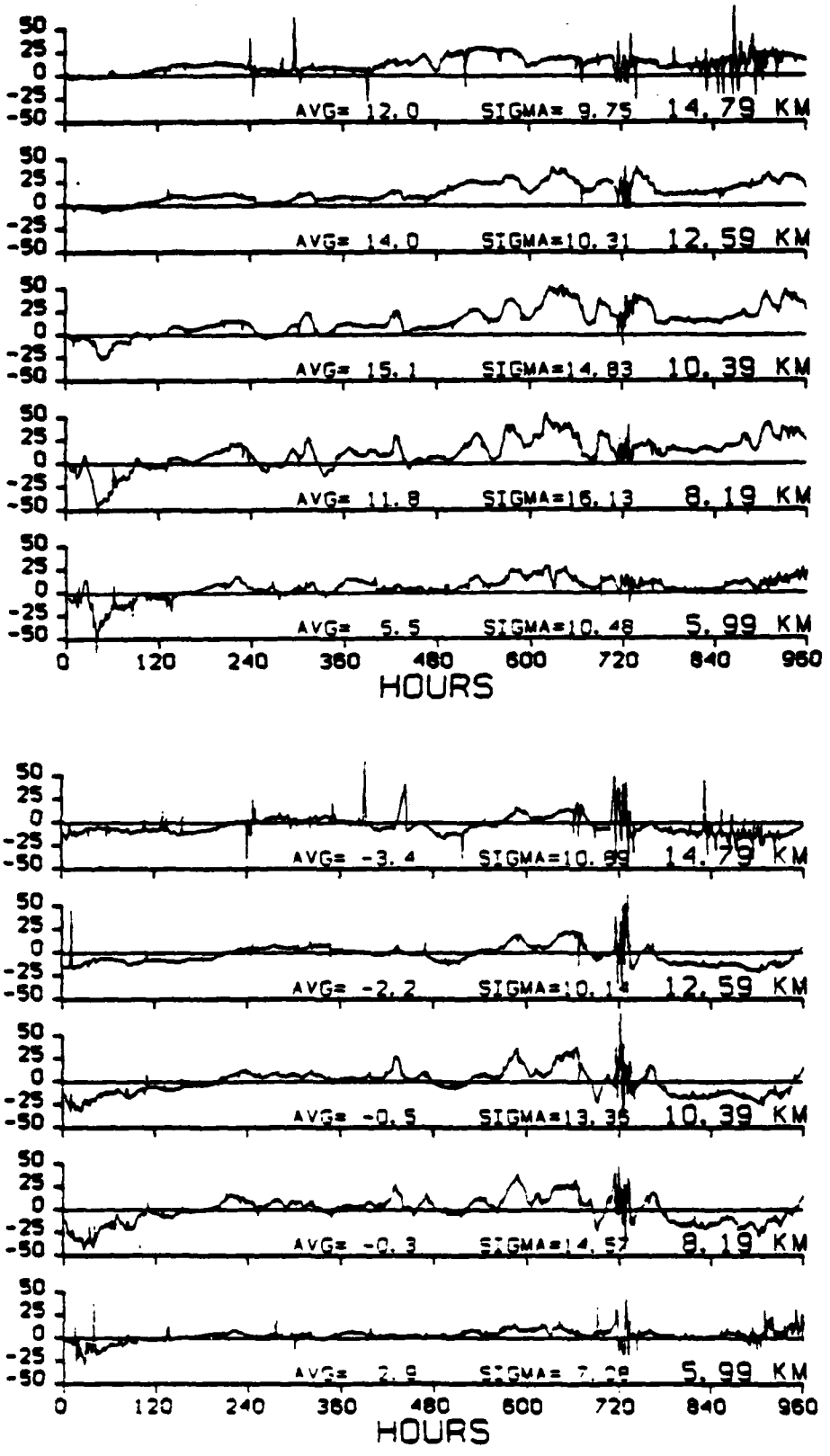

FIG. 1. The original data set of 960 hourly values at each of the five heights used in the study are shown as function of time. The average value and the variance at each of the heights are shown. The top half of the figure is for the zonal wind component, and the bottom half shows the meridional component.

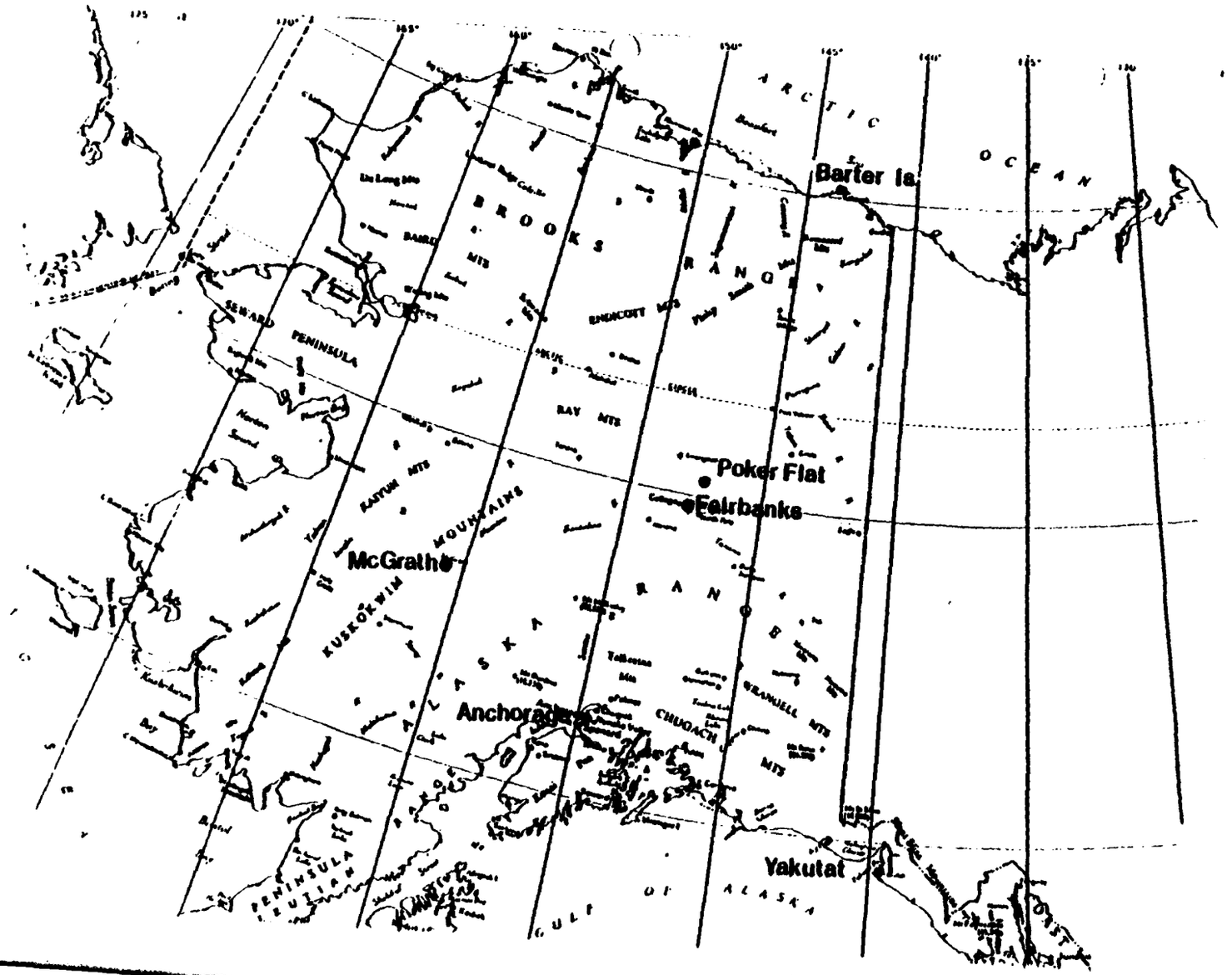
Barter Is.
Poker Flat
Fairbanks
McGrath
Anchorage
Yakutat
ARCTIC OCEAN
BROOKS RANGE
SEWARD PENINSULA
KUSKOKWIM MOUNTAINS
ALASKA RANGE
CHUGACH MTS
WRANGELL MTS
GULF OF ALASKA

MARCH 1 - APRIL 1, 1979

1 HR. AVG. RADAR WINDS VS. SINGLE RAWINSONDE PROFILE

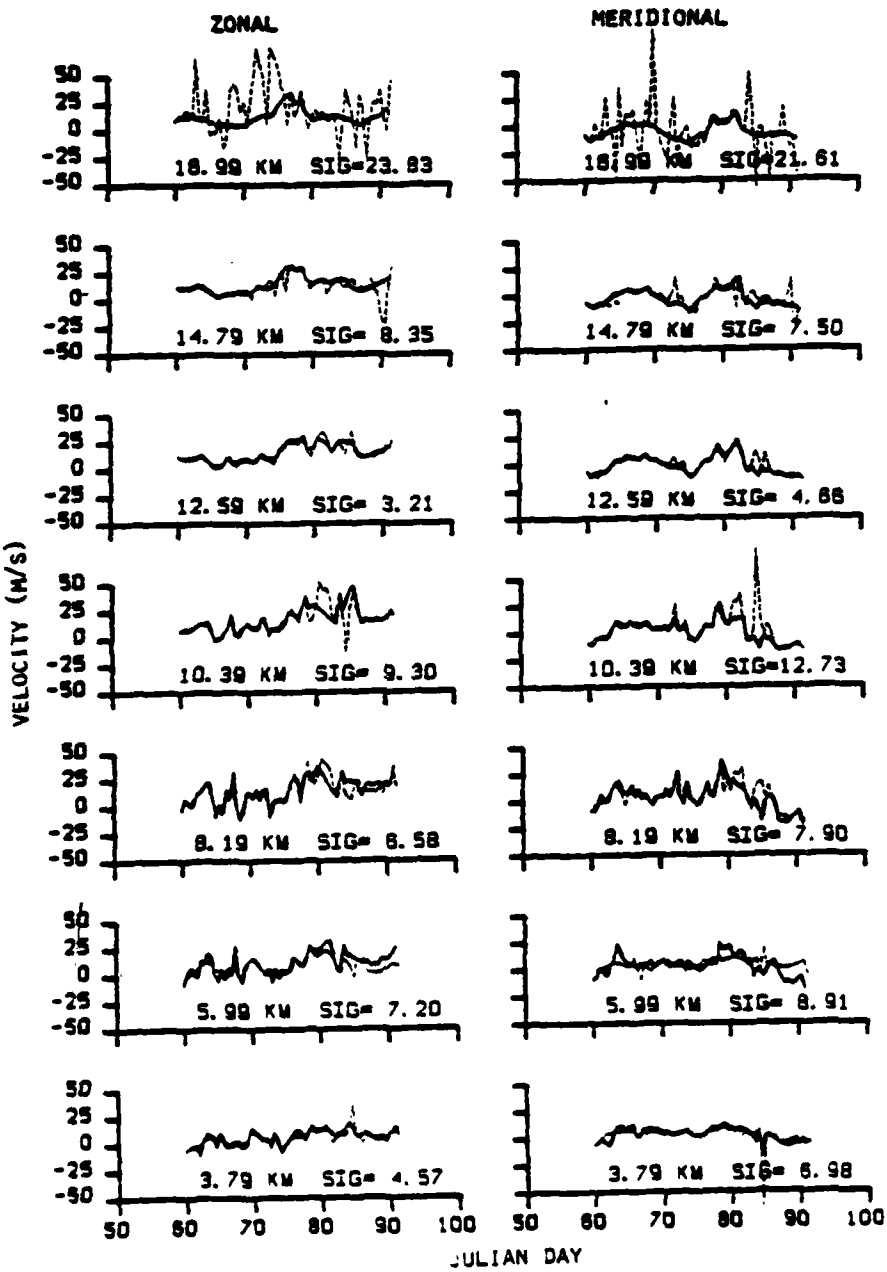

Figure 3

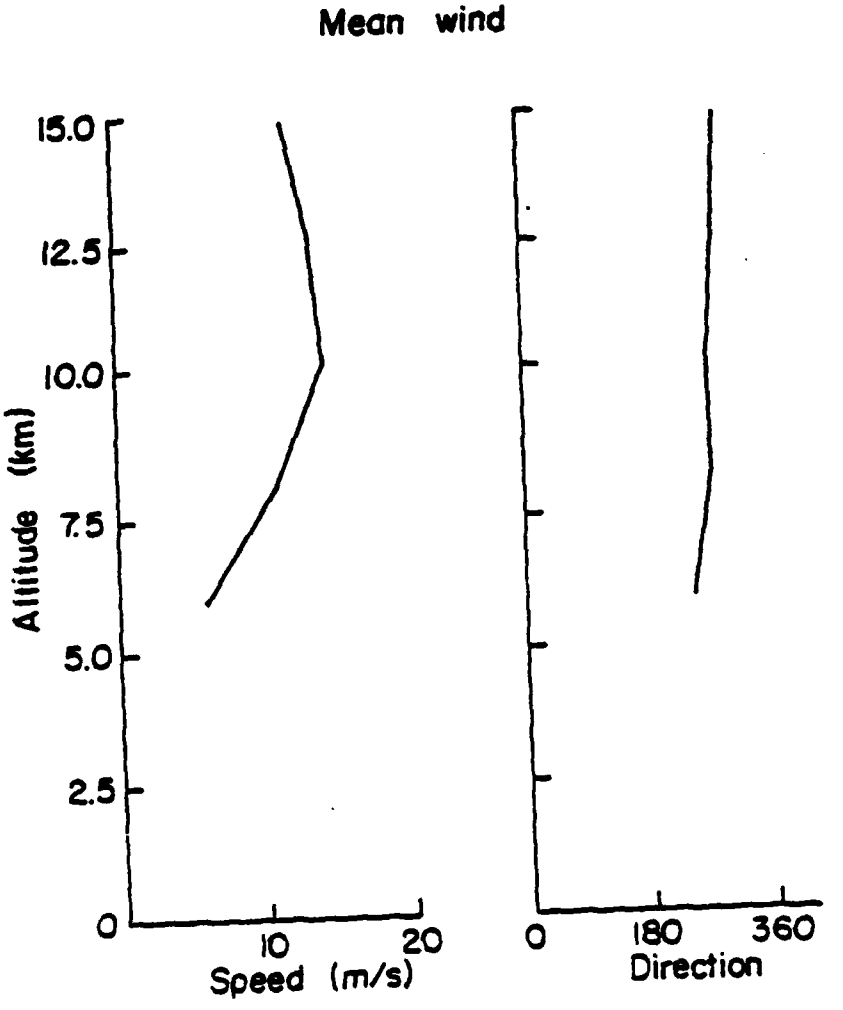
Mean wind
15.0
12.5
10.0
7.5
5.0
2.5
0
Altitude (km)
10
20
Speed (m/s)
0
180
360
Direction

Figure 4

MARCH 1 - APRIL 1, 1979

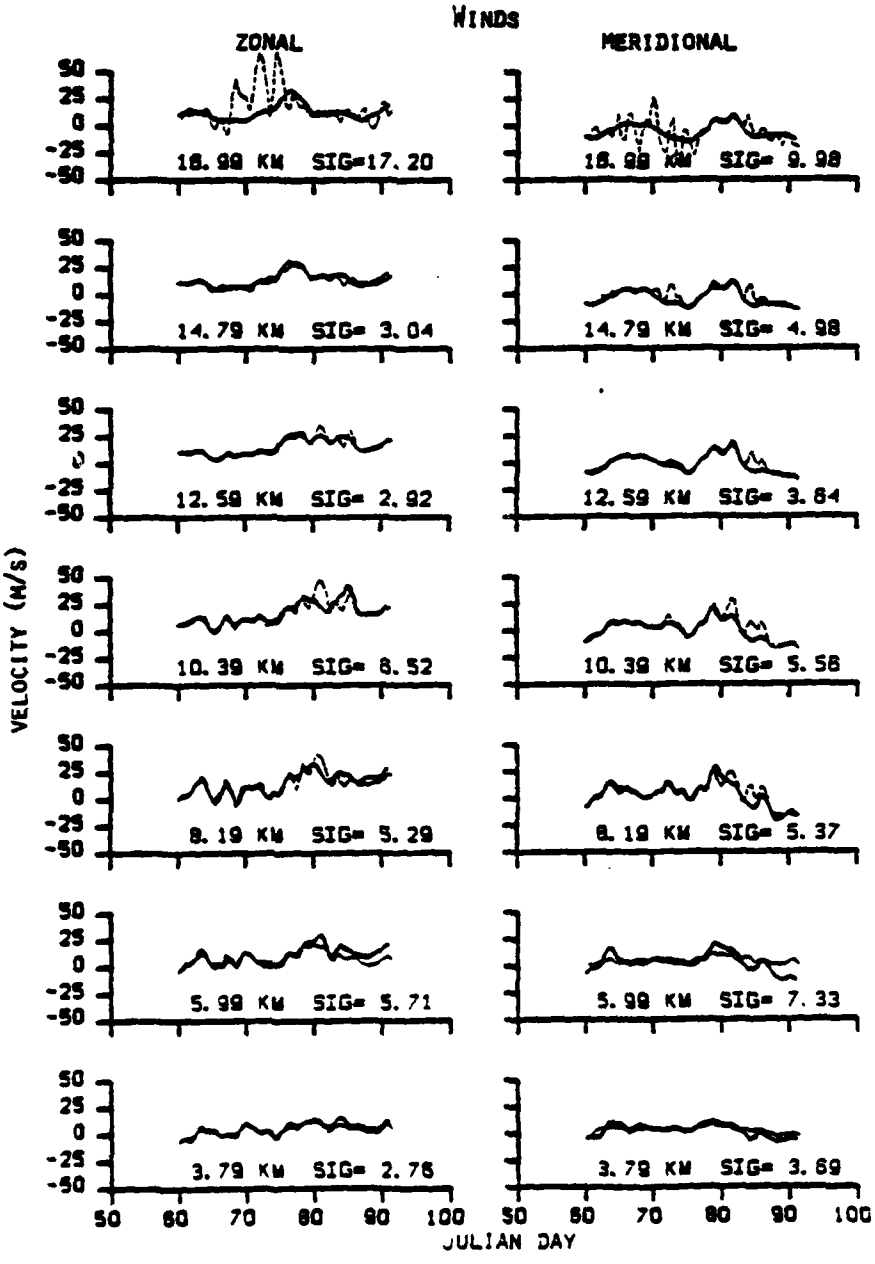

Figure 5

MARCH 1 - APRIL 1, 1979

12 HR. AVG. RADAR WINDS VS. SINGLE RAWINSONDE PROFILE

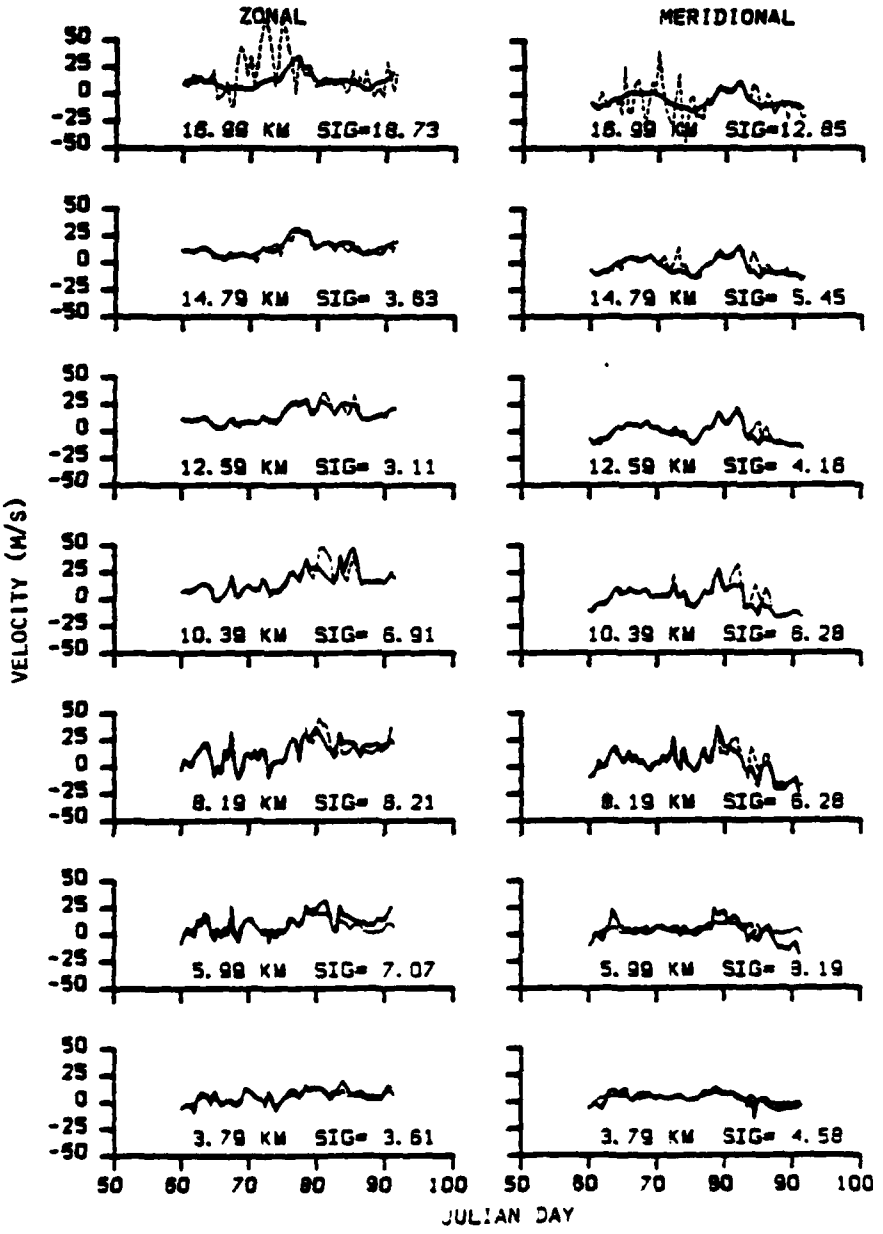

Figure 6

MARCH 1 - APRIL 1, 1979

24 HR. AVG. RADAR WINDS VS. CRESSMAN ANALYSIS (R=750 KM)

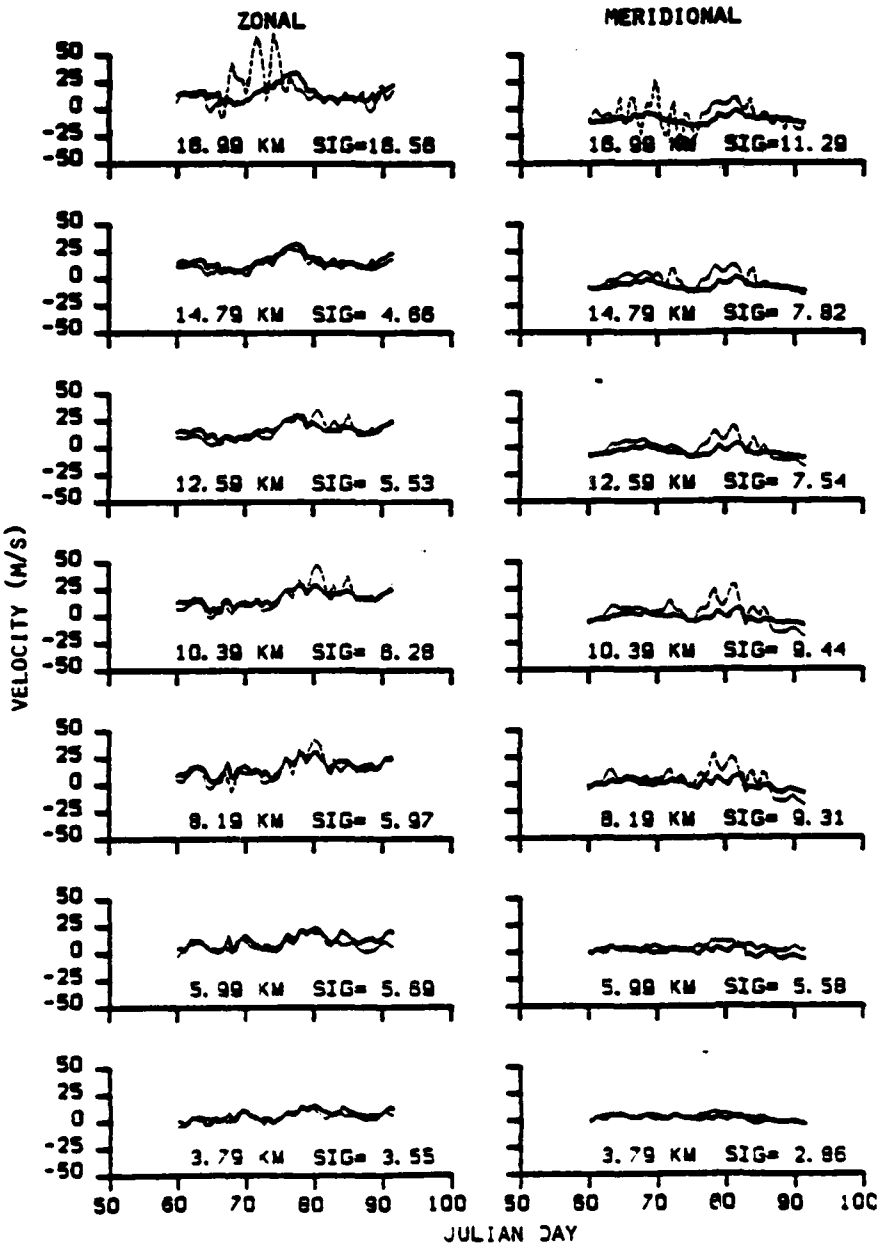

Figure 7

MARCH 1 - APRIL 1, 1979

24 HR. AVG. RAWINSONDE WINDS VS.

CRESSMAN ANALYSIS (R=750 KM)

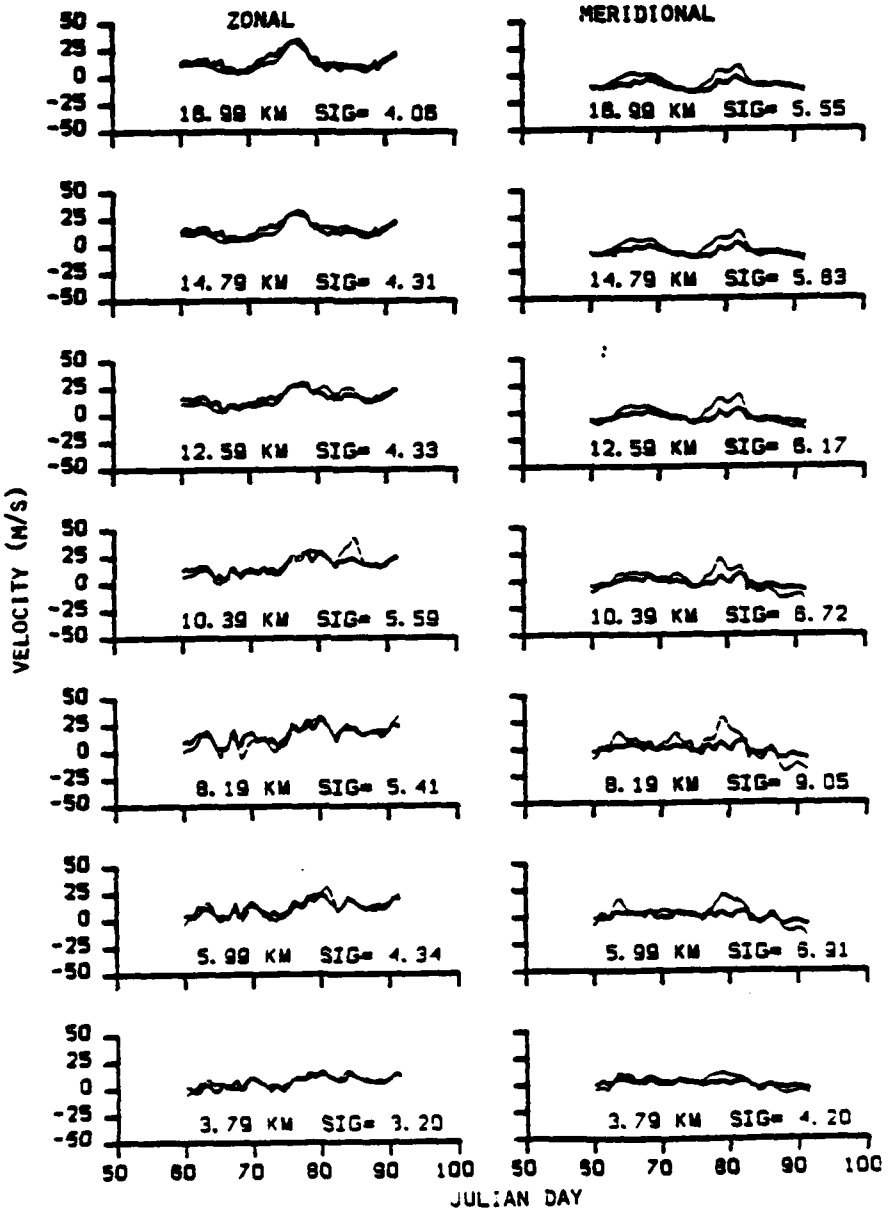

Figure 8

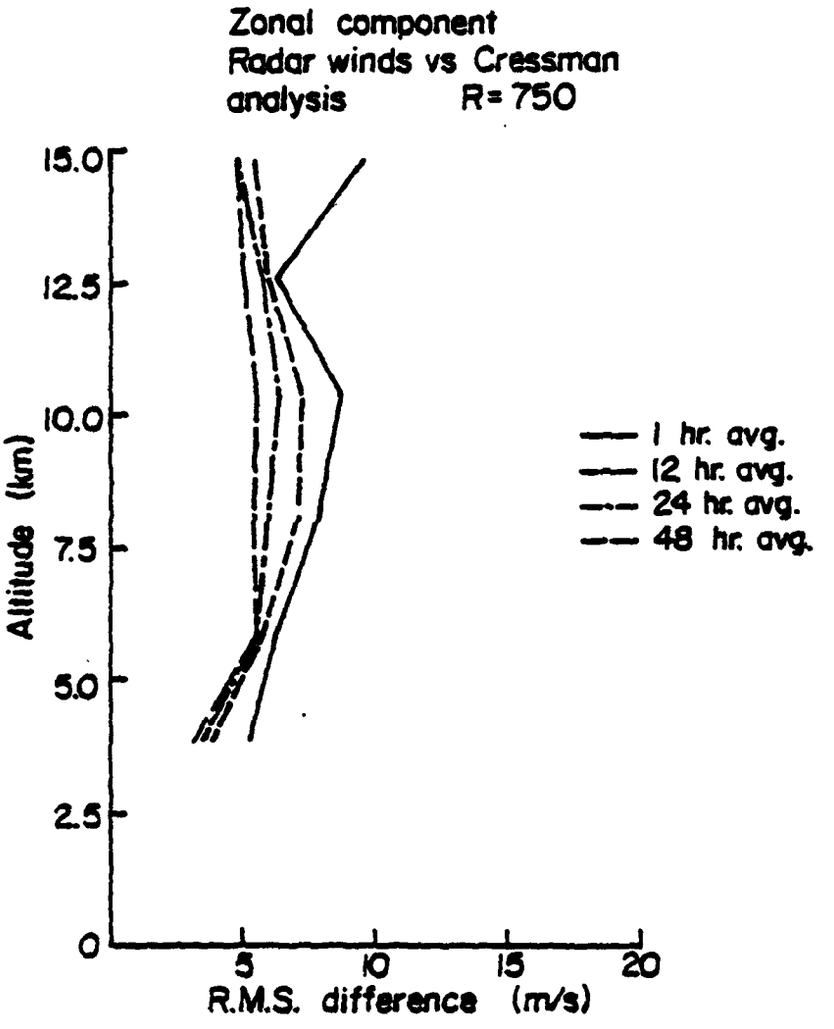
Zonal component
Radar winds vs Cressman
analysis R=750
15.0
12.5
10.0
7.5
5.0
2.5
0
Altitude (km)
5
10
15
20
R.M.S. difference (m/s)
1 hr. avg.
12 hr. avg.
24 hr. avg.
48 hr. avg.

Figure 9a

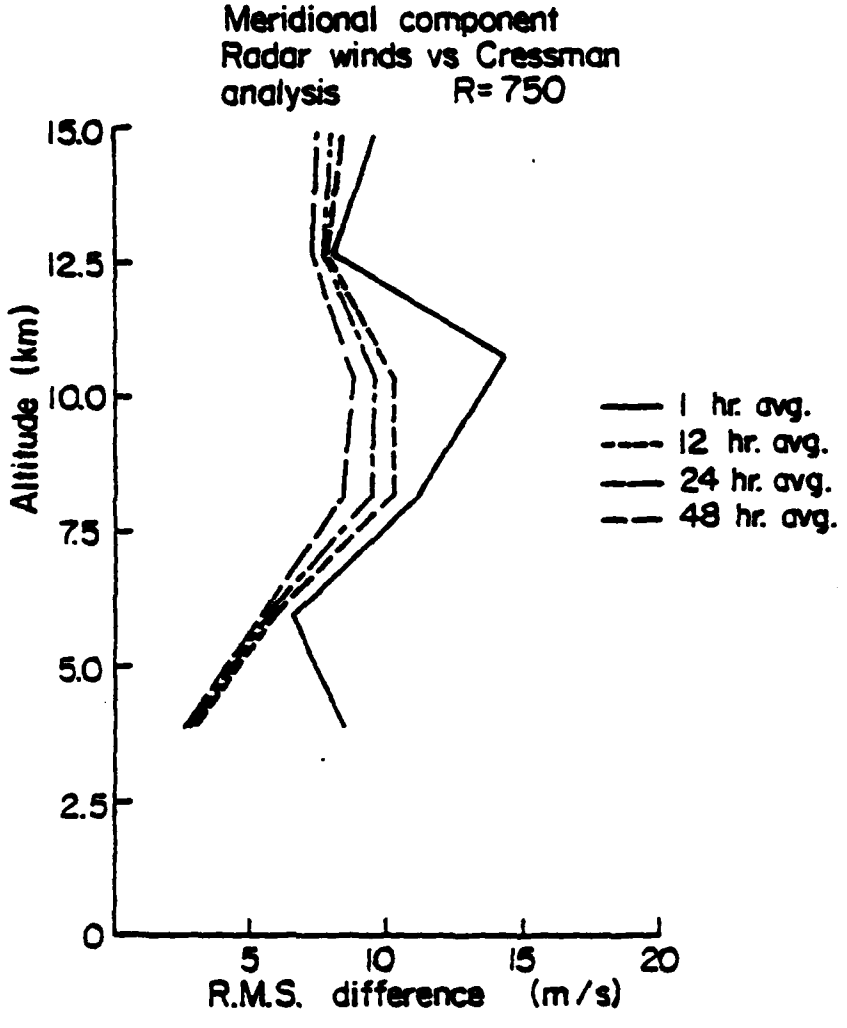
Meridional component
Radar winds vs Cressman
analysis R=750
15.0
12.5
10.0
7.5
5.0
2.5
0
Altitude (km)
5
10
15
20
R.M.S. difference (m/s)
1 hr. avg.
12 hr. avg.
24 hr. avg.
48 hr. avg.

Figure 9b

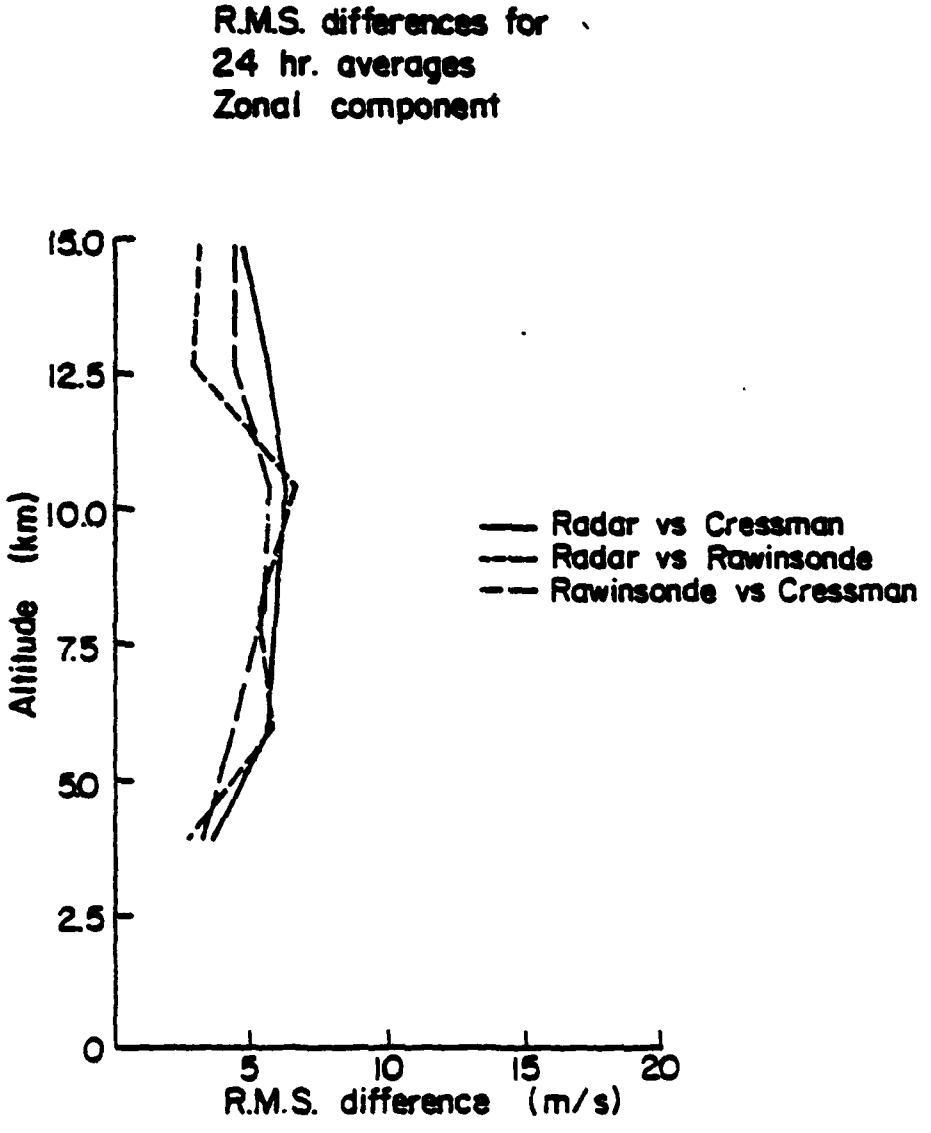
R.M.S. differences for
24 hr. averages
Zonal component
15.0
12.5
10.0
7.5
5.0
2.5
0
Altitude (km)
5
10
15
20
R.M.S. difference (m/s)
Radar vs Cressman
Radar vs Rawinsonde
Rawinsonde vs Cressman

Figure 10a

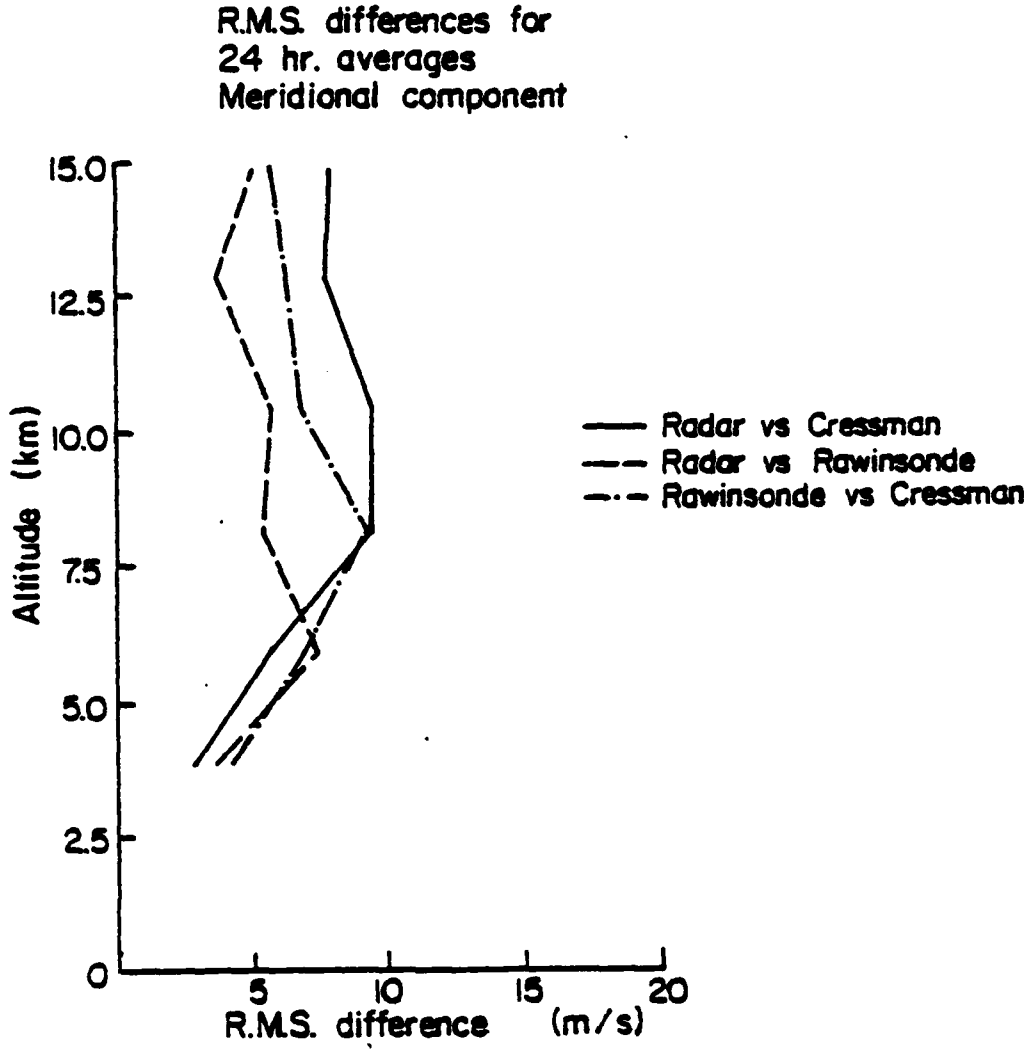
R.M.S. differences for
24 hr. averages
Meridional component
15.0
12.5
10.0
7.5
5.0
2.5
0
Altitude (km)
5
10
15
20
R.M.S. difference (m/s)
Radar vs Cressman
Radar vs Rawinsonde
Rawinsonde vs Cressman

Figure 10b

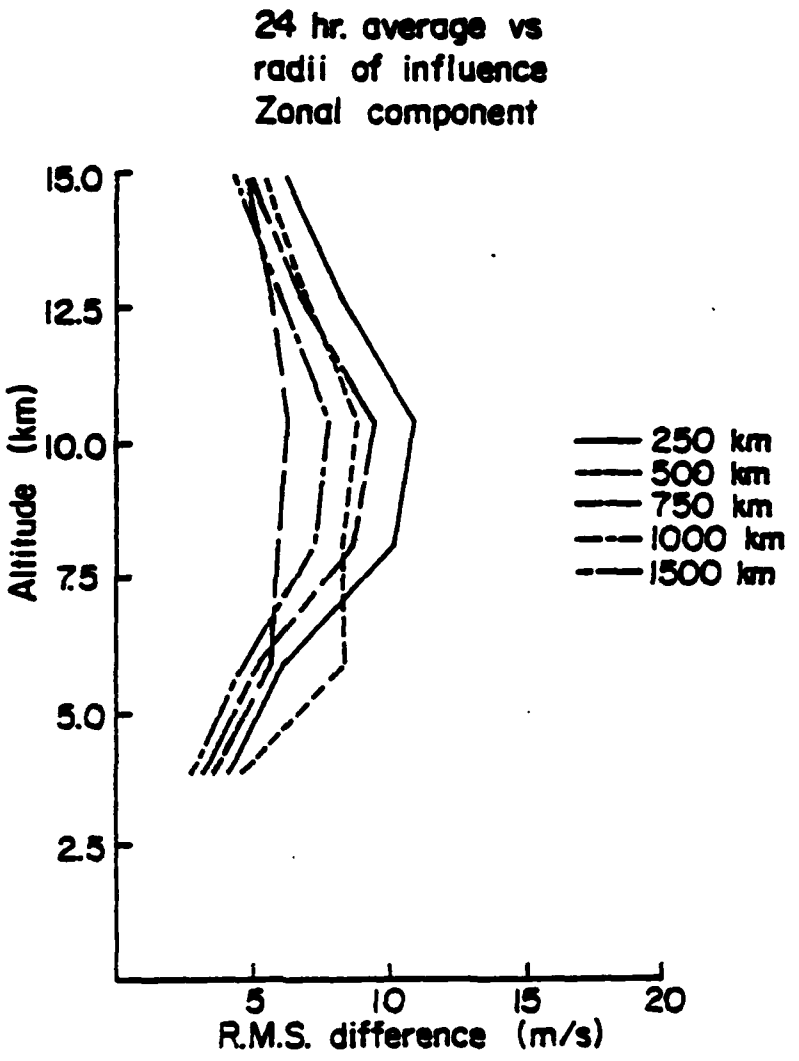
24 hr. average vs
radii of influence
Zonal component
15.0
12.5
10.0
7.5
5.0
2.5
Altitude (km)
5
10
15
20
R.M.S. difference (m/s)
250 km
500 km
750 km
1000 km
1500 km

Figure 11a

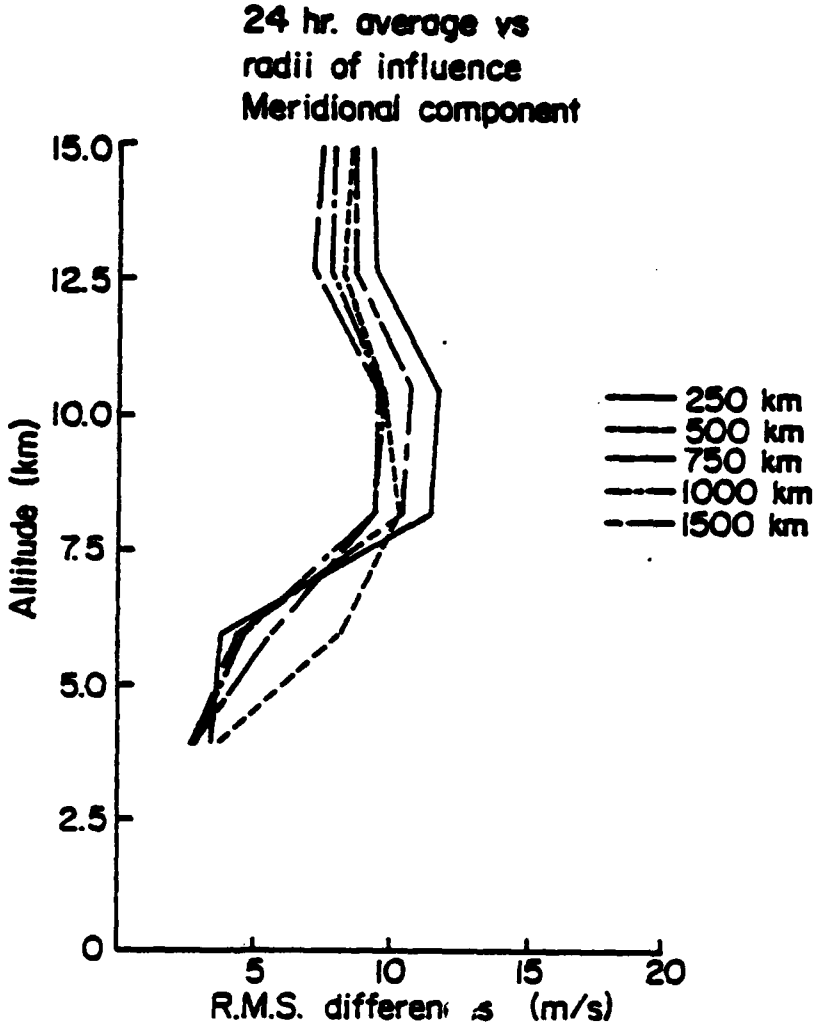
24 hr. average vs
radii of influence
Meridional component
15.0
12.5
10.0
7.5
5.0
2.5
0
Altitude (km)
5
10
15
20
R.M.S. differences (m/s)
250 km
500 km
750 km
1000 km
1500 km

Figure 11b

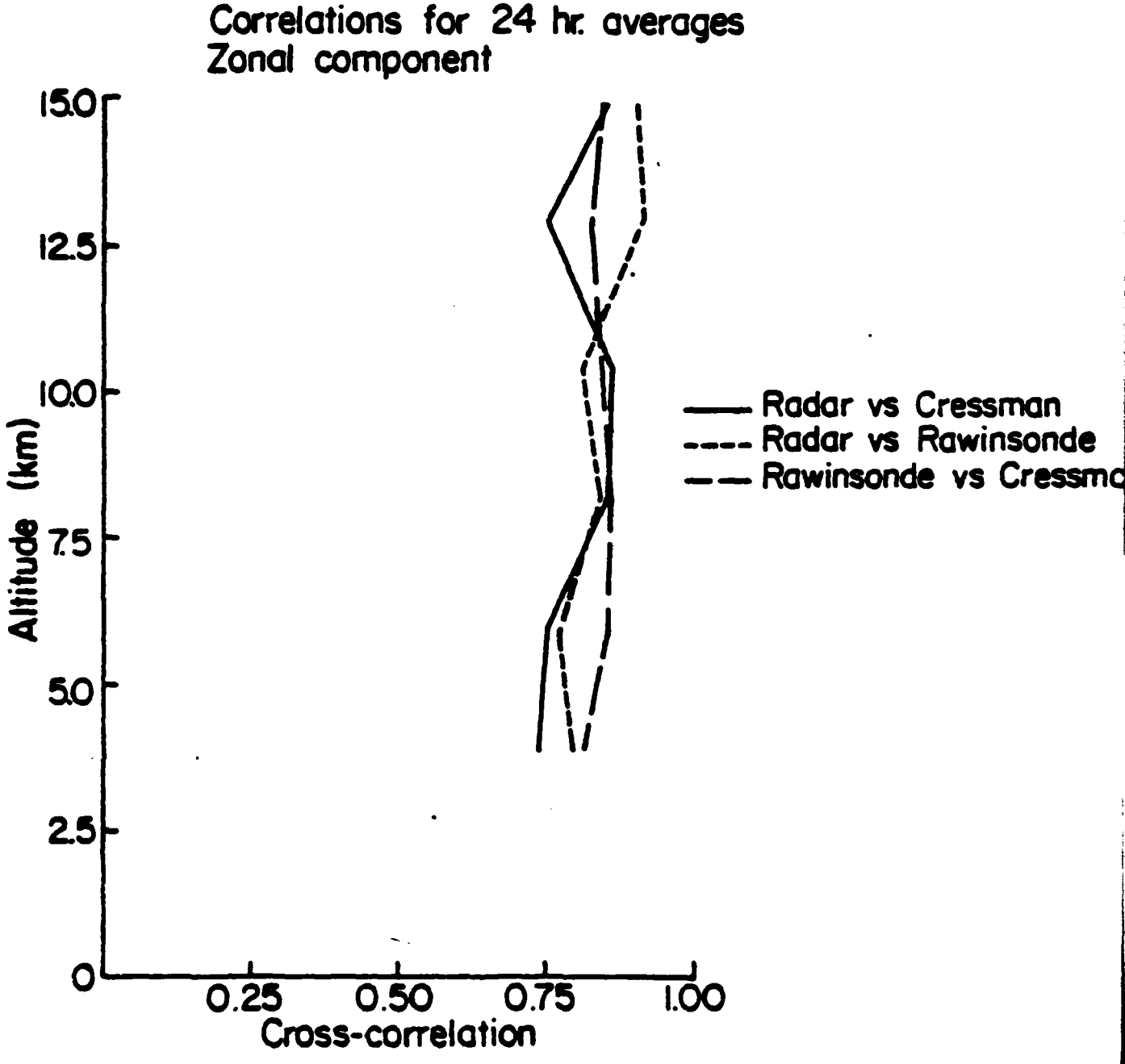
Correlations for 24 hr. averages
Zonal component
15.0
12.5
10.0
7.5
5.0
2.5
0
Altitude (km)
0.25
0.50
0.75
1.00
Cross-correlation
Radar vs Cressman
Radar vs Rawinsonde
Rawinsonde vs Cressma

Figure 12

APPENDIX III

[Reprinted from BULLETIN OF THE AMERICAN METEOROLOGICAL SOCIETY, Vol. 63, No. 9, September 1982]
Printed in U. S. A.

VHF and UHF Doppler Radars as Tools for Synoptic Research

M. F. Larsen and J. Röttger

VHF and UHF Doppler Radars as Tools for Synoptic Research

M. F. Larsen[1] and J. Röttger[2]

Abstract

Applications of VHF and UHF Doppler radars to research in synoptic meteorology are reviewed. We find that these radars show great potential for studies of large scales, but the area of research where the instruments really excel is in studying the interaction between the synoptic scale and the mesoscale. Several examples of results in both these areas are presented. Finally, the potential for operational use of the radar systems is discussed.

1. Introduction

Sensitive VHF and UHF Doppler radars are providing a powerful new tool for investigations of the dynamics of the atmosphere at small scales typically associated with gravity waves and 3-dimensional turbulence. VHF is characterized by wavelengths between 10 m and 1 m, and UHF corresponds to the range from 1 m to 10 cm. The radars measure the winds by detecting backscatter from turbulent variations in the refractive index, i.e., humidity, temperature, and density variations. The measurement technique and many of the observations have been described by Gage and Balsley (1978), Balsley and Gage (1980), Röttger (1980), and Harper and Gordon (1980). Many of these coherent radars have high power transmitters and large antennas that enable them to detect the small backscattered power to altitudes in the stratosphere and mesosphere. The great sensitivity of the radars makes it feasible to obtain wind profiles with height and time resolution of the order of 100s of meters and minutes, making the technique a natural candidate for investigations of relatively small-scale phenomena. Indeed, a great deal of light is already being shed on the dynamics of the microscale in the troposphere and lower stratosphere, something about which little is known. It is only within the past few years that the usefulness of the radar data for applications in synoptic meteorology has become apparent. Because the topic has not been discussed fully in the past, we shall concentrate on this aspect.

The excellent time and height resolution afforded by the radars make them an excellent tool for investigating microscale dynamics. However, these same features are no less valuable for studies of larger scales. The high time resolution means that a better estimate of the wind over longer time scales is possible when the influence of the variability over short time scales can be eliminated by averaging. Rawinsonde data are not necessarily representative of the mean wind over the 12 h period between successive balloon launches. The radars also have the unique capability of measuring vertical velocities with great accuracy and good time resolution on a routine basis. Although vertical velocity measurements can be made by other techniques, the radars cannot be rivaled, as far as observing for long periods is concerned. Since so much of synoptic meteorology involves the prediction of vertical velocities, this facet makes the radar a valuable asset to the field in and of itself. It also has been discovered that meter-wavelength radars are capable of detecting inversions in the temperature profile. Enhanced reflections occur at a level just above the beginning of an inversion; this is providing valuable information about the height of the tropopause, as well as an interesting view of the structure of frontal systems.

The exchange of air between the stratosphere and troposphere at mid-latitudes occurs primarily in association with the tropopause folding mechanism that occurs at the junction between the cold-frontal surface and the troposphere. The intrusions of stratospheric air occur in regions with a horizontal scale of a few hundred kilometers and a vertical scale of 1 km (Holton, 1981). The radar measurements have the height resolution necessary to study this process in detail and provide the vertical velocity measurements that are needed to understand the dynamics of mixing across the tropopause.

All the topics mentioned above are far from being completely explored. Most of the areas of investigation are still in their infancy. However, the results to date already indicate the potential of the UHF and VHF Doppler radars for synoptic research and for studies of the interaction between the synoptic and mesoscale. In this review we shall present what we believe are some of the more interesting results of recent investigations in the field and discuss some of the possibilities for future research. We shall also touch on the feasibility of operational use of the radars.

2. The measurement technique

The general features of Doppler radar velocity measurements have been described by others (e.g., Wilson and Miller, 1972; Battan, 1973; Doviak *et al.*, 1979). We shall not review the basic theory (See Balsley and Gage (1982) in this issue for a complete review) but merely describe the particular aspects of the problem that relate to the UHF and VHF radars. The

[1] School of Electrical Engineering, Cornell University, Ithaca, N.Y. 14853.
[2] EISCAT Scientific Association, Box 705, S-98127 Kiruna, Sweden. On leave from Max Planck Institüt für Aeronomie, 3411 Katlenburg-Lindau 3, Federal Republic of Germany.

0003-0007/82/090996-13$07.25

pulsed Doppler radars emit either a single pulse or a train of pulses of electromagnetic radiation, and some of the energy is backscattered when variations in the refractive index structure of the atmosphere at scales of half the radar wavelength are encountered. By measuring the frequency of the returned signal, the small change in frequency due to the motion of the scatterers can be determined. The Doppler shift in frequency can then be related directly to the line-of-sight velocity of the turbulent variations in the refractive index. If the turbulent variations are "frozen" in the medium during the time it takes to cross the radar beam (the Taylor hypothesis), the Doppler velocity is then a measure of the mean motion of the atmosphere over the volume that the radar illuminates.

The accuracy of the radar-deduced winds has been tested by comparisons of radar wind profiles and rawinsonde profiles from nearby stations (Balsley and Farley, 1976; Farley *et al.*, 1979; Strauch, 1981). However, a comparison between the measurements of a 6 m and a 3 cm radar also has been carried out (Strauch *et al.*, 1982). The microwave radar makes wind measurements indirectly by measuring the velocity of precipitating particles, but it is highly accurate, particularly when snow is present. The comparisons were carried out under the appropriate conditions and good agreement was achieved, thus circumventing the problem that usually arises when the radar measurements are compared to rawinsonde measurements. The agreement is usually good, but not perfect, and the differences are then attributed to variations over the spatial separation between the balloon ascent and the radar facility.

Given that the line-of-sight velocities can be obtained, there are three methods in use for determining the vector winds. The first is the VAD (velocity azimuth display) technique in which a steerable antenna beam, pointed at some angle off zenith, is used to measure the line-of-sight velocity as a function of azimuth and height (Lhermitte and Atlas, 1963; Wilson and Miller, 1972). If the winds do not vary over the cone traced out by the beam, and the velocity is strictly horizontal, the velocity measured by the radar will vary sinusoidally as a function of the azimuth. A nonzero vertical velocity component will create an offset in the sinusoid. The main advantage of the VAD technique is that in theory at least, variations of the winds over the sampling cone due to divergences or rotations in the wind field also can be resolved by this technique if more Fourier components than just the first order sinusoid are included in the fit. In spite of this advantage, the information has not really been put to practical use in any of the experiments that we are aware of. The other two techniques described next require the assumption of homogeneity in the wind over the spatial separation of the beams in order to resolve the vector wind. The major disadvantage of the VAD technique is that the need for a steerable dish antenna puts a practical limit on the antenna size.

The second method of determining the vector wind is to use a fixed dipole array (Woodman and Guillen, 1974). By phasing the signal fed to the various parts of the array, the transmitted beam can be moved off vertical. The vector wind can be determined uniquely by pointing beams in three different directions in what amounts to a simplified VAD technique. Usually one beam is pointed in the vertical direction and two in the off-vertical direction at an angle of 5° to 15°. The Poker Flat MST (Mesosphere, Stratosphere, Troposphere) radar is operated in this configuration, for example (Balsley *et al.*, 1980). The main advantages of this type of system are that the antenna is easy to construct and relatively inexpensive. Also, antenna arrays with dimensions as large as 200 m × 200 m can be utilized, something that would be very difficult with a steerable dish system. The disadvantages are that for large antennas, considerable real estate is involved

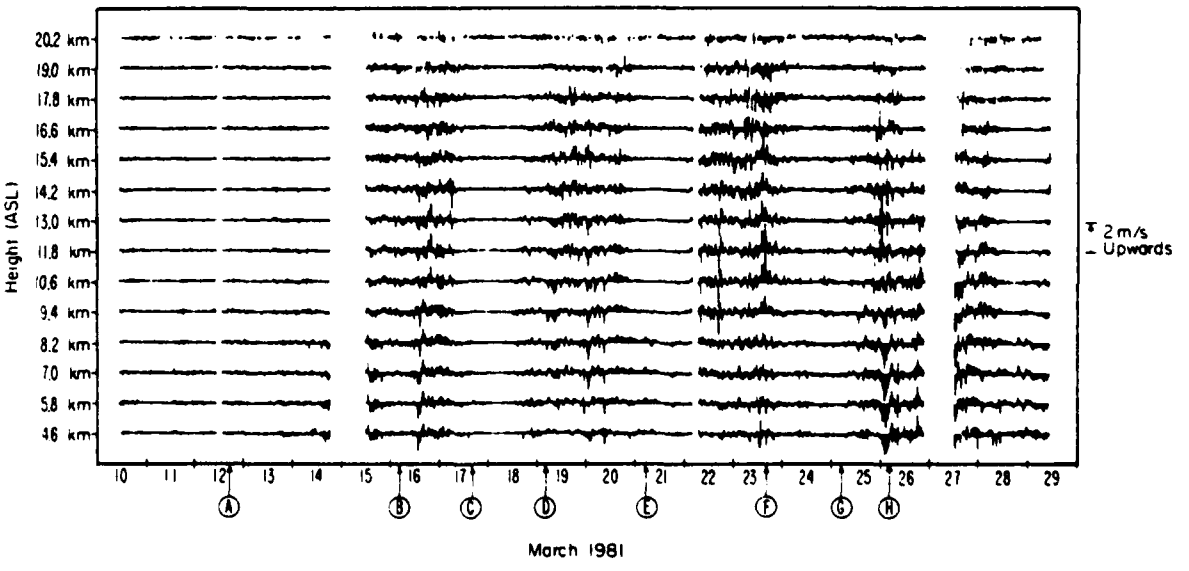

FIG. 1. Vertical velocities measured with the Platteville, Colo., 50 MHz radar. The reference scale is shown at the right-hand axis. The time series covers a period of 19 days, and the height resolution is 1.2 km. Alternating quiet and active periods repeat every four to five days.

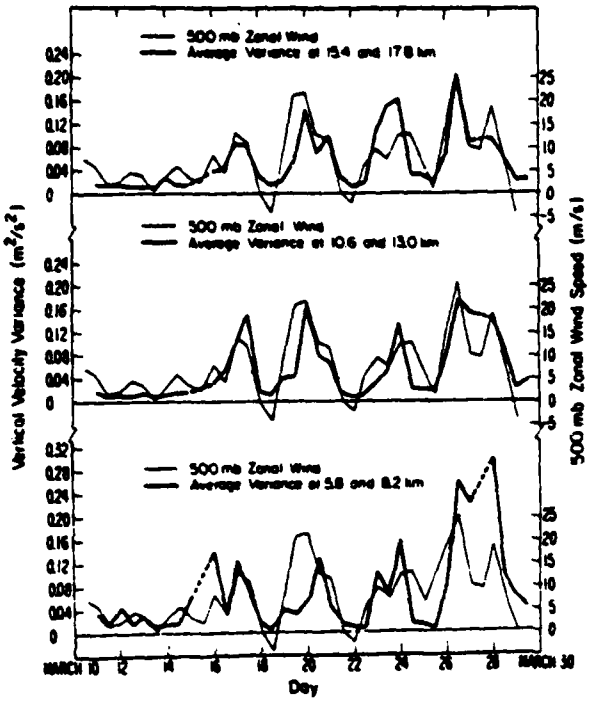

FIG. 2. Average variance in the vertical velocity at 15.4 and 17.8 km for the data shown in Fig. 1 compared to the 500 mb zonal wind measured by the Denver radiosonde. The variance was calculated for a 2 h period centered on the time of the radiosonde ascent.

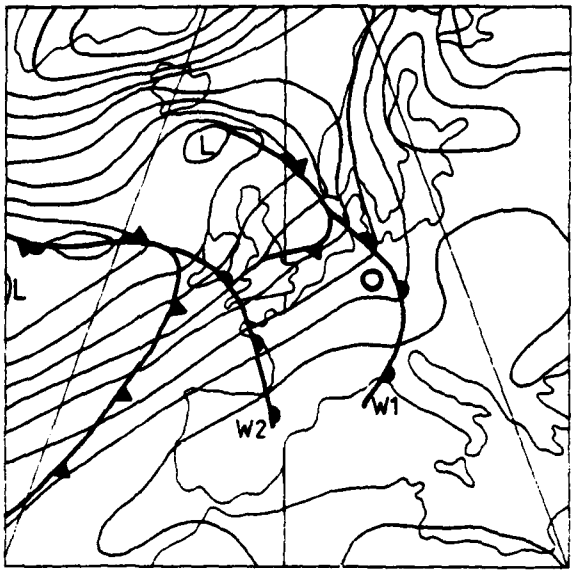

FIG. 3. Synoptic situation at 0000 GMT on 7 March 1981. The heavy circle shows the location of the SOUSY-VHF-radar. The radar data taken during the passage of the warm front labeled W2 are shown in Fig. 4.

and there is no way to take into account variations in the wind field over the distance separating the beams. The latter has not been a problem except during strong gravity wave events.

The third technique is the spaced antenna (SA) measurement advocated by Röttger and Vincent (1978) and Vincent and Röttger (1980). The capabilities of the SA method were compared to the two methods described above by Briggs (1980) and Röttger (1981a). For this method one transmitter array and three spatially separated receiver arrays are used. The horizontal wind components are determined by a correlation analysis of the signals measured at the three receiver arrays. The vertical velocity is found from the Doppler-shift of the radar echoes. As mentioned in the introduction, radars are particularly sensitive to temperature inversions and other stratified structures such as fronts. It has been determined that there is an enhanced reflectivity for radars operating at wavelengths of the order of meters when the radar beam is pointed vertically and that the returned power drops off very rapidly within a few degrees of vertical. Since the SA technique uses only vertically pointing beams, it is possible to detect echoes with a higher signal-to-noise ratio than those that could be detected with a system using an off-vertical beam configuration. The disadvantages of the SA method are essentially the same as those of the fixed dipole array method. Perhaps the SA radar handles inhomogeneities in the sampling volume slightly better than the Doppler method since the measurement, by its very nature, tends to average variations in the atmospheric structure between the two receiving antennas. Also, the vertical velocities can be measured in all three receiving beams simultaneously and this provides direct information on the spatial variations within the sampling volume.

The layered structures that enhance the reflectivity at vertical incidence may not be moving with the wind speed but may be modulated by waves or the slope of frontal surfaces, as we shall discuss later. In such cases, the measured vertical velocity will have a contribution both from the effect of the sloped surface as it moves through the beam and the real vertical wind. With three beams and good height resolution, the orientation of the layers can be determined. The vertical velocity measurements can then be corrected for this effect (See Appendix in Röttger, 1981c).

3. Modulation of vertical velocity fluctuations by planetary waves

Ecklund *et al.* (1981a,b) have used the Poker Flat, Alaska,

FIG. 4. a) Reflectivity contour plot. Difference between contour lines is 2 dB. Intensity of shading corresponds to intensity of echoes. b) Contour plot of vertical velocities. Shading indicates downward velocity. The interval between contours is 7.5 cm/s. c) Contour plot of wind speed with a contour interval of 2.5 m/s. Shading indicates speeds greater than 20 m/s. The heavy stippled areas correspond to missing wind data due to undersampling. d) Thermal structure and winds near fronts adapted from Palmén and Newton (1969). The heavy line labeled TP corresponds to the height of the tropopause. The dashed lines are the isotherms, and the solid lines are the isotachs. The jet is located on the warm side of the front just below the tropopause.

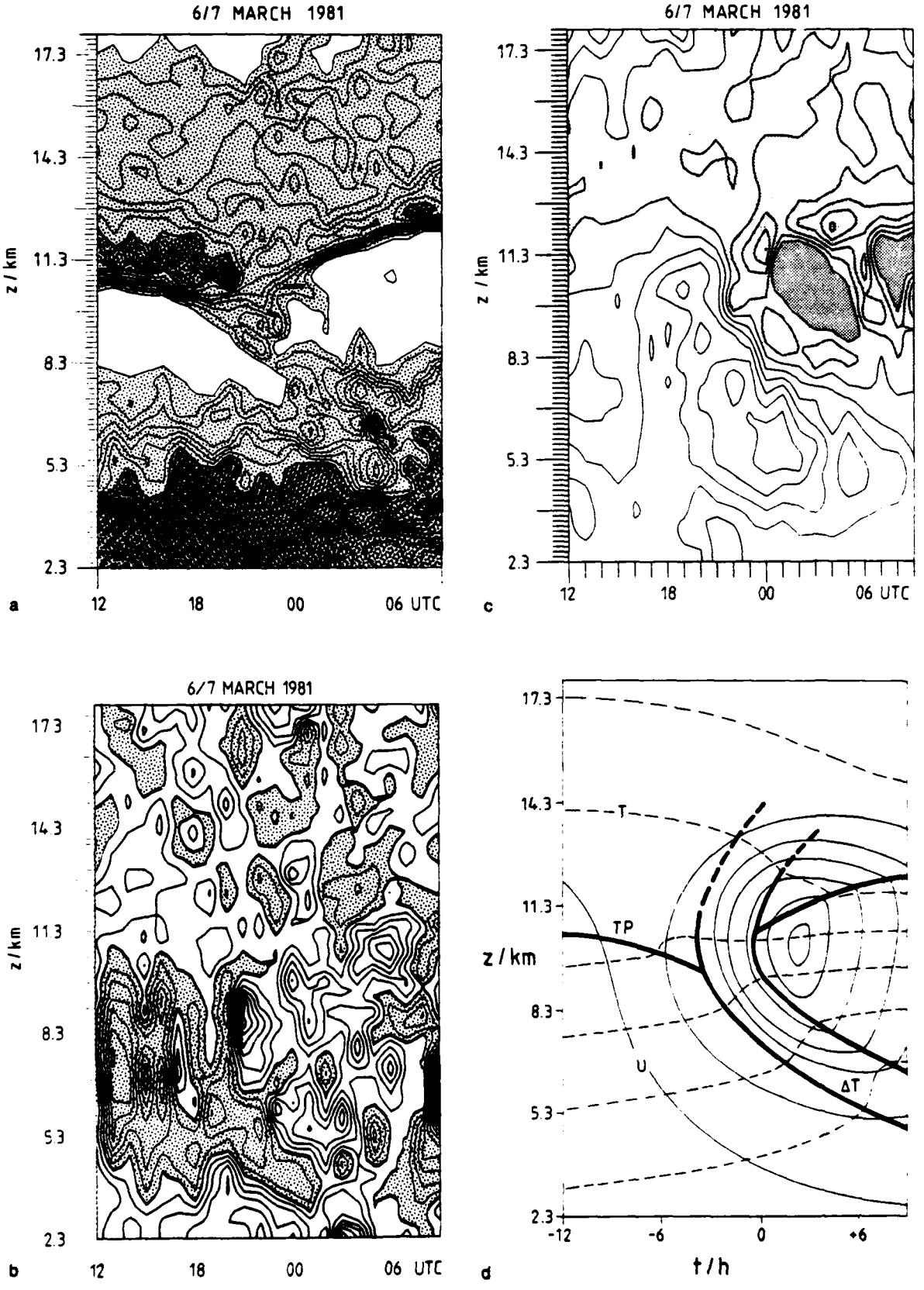
6/7 MARCH 1981
17.3
14.3
11.3
8.3
5.3
2.3
z / km
12
18
00
06 UTC
a
6/7 MARCH 1981
17.3
14.3
11.3
8.3
5.3
2.3
z / km
12
18
00
06 UTC
c
6/7 MARCH 1981
17.3
14.3
11.3
8.3
5.3
2.3
z / km
12
18
00
06 UTC
b
17.3
14.3
11.3
8.3
5.3
2.3
z / km
T
TP
U
ΔT
-12
-6
0
+6
t / h
d

MST radar and the Platteville, Colo. radar, both of which operate at a frequency of 50 MHz, to study the nature of vertical velocity fluctuations over periods of several weeks. The 15 min. average vertical velocities for a three-week period in March at Platteville are shown in Fig. 1. It is evident that there are several days of low activity followed by 3 or 4 days of high activity. This pattern repeats during the observations. The period of the envelope modulating the vertical velocity variability is similar to the period of planetary-scale waves. Ecklund *et al.* (1981b) found that the 500 mb synoptic maps for the period indicated that the levels of high activity corresponded to periods when a strong zonal flow was present. This is shown more clearly in Fig. 2, which shows the vertical velocity variance at three different heights plotted together with the 500 mb zonal wind speed. There is clearly a good correlation between the two. The explanation by Ecklund *et al.* (1981b) was simply that it was an orographic effect associated with the mountains west of Platteville. The stronger the zonal flow, the larger the amplitude of the vertical velocity fluctuations associated with the gravity waves generated in the lee of the mountains.

Observations have been made simultaneously with the Platteville radar and the Sunset 50 MHz radar located in the mountains west of Boulder (Balsley *et al.*, 1981). Corresponding active and quiet periods were seen at both locations, but it was found that the magnitude of the variance at Sunset, located in the mountains, was much greater than that at Platteville, located on the plains east of the mountains.

It has long been known that the Continental Divide exerts a drag on the planetary-scale flow. General circulation models usually include some parameterization scheme to simulate this effect in order to make the simulations more realistic. The variance in the vertical velocities observed at Platteville and Sunset are indicators of the amount of damping of the zonal flow that is taking place. The energy taken out of the flow manifests itself as small-scale eddies or gravity waves. The fluctuations observed at Platteville should be particularly useful for estimating the damping, since the location is in the lee of the mountains.

The study by Ecklund *et al.* (1981a) showed a similar variability in the vertical velocity fluctuations at Poker Flat, with quiet and active periods alternating every 3 to 4 days. However, the implications of that study were slightly different. The terrain surrounding the Alaska site is not as well defined as that at Platteville. Indeed, no clear relationship that would indicate an orographic effect could be found between the direction or magnitude of the wind and the degree of activity. The strongest correlation was found when the average wind shear between 3.9 and 19.7 km altitude was plotted against the vertical velocity variance. The agreement between the two curves is not as good as that in Fig. 2, but there is enough similarity to raise the possibility that a dynamic interaction between the large-scale planetary waves and the short-period gravity wave oscillations accounted for the modulation pattern. A similar result was reported by Röttger (1981a). This effect will have to be examined in more detail to determine if such a relationship exists.

If it can be determined that planetary waves do modulate short period fluctuations in the vertical velocities, the radar measurements of vertical velocities could be important in understanding of how the synoptic and meso-scales interact. This would appear to offer a great potential for application of the radar technique. Klostermeyer (1981) has discussed the application of the technique to other studies of the interaction of different scales.

The time series in Fig. 1 show that some averaging will certainly be necessary if the mean vertical velocity measured by the radars is to be representative of the synoptic situation. It is still to be determined if effects due to wave perturbations can be averaged out in such a way that the result is meaningful. G. Nastrom (personal communication, 1982) is presently investigating these questions by comparing the long time series of vertical velocities measured by the Poker Flat MST radar with the vertical velocities derived from radiosonde data using the quasi-geostrophic ω equation and other techniques.

4. Observations of frontal passages

Röttger (1979) and Röttger and Schmidt (1981) have made observations of warm frontal passages with the SOUSY/VHF radar located in the Harz mountains in Germany. Figure 3 shows the synoptic situation at 0000 GMT on 7 March 1981. The location of the SOUSY radar is indicated by a heavy circle. The map shows that the area was affected by two lows, one centered near Iceland and the other centered due west of England. Each low is characterized by a distinct set of fronts. The warm front labeled W1 shows signs of occlusion, as does the one labeled W2. Radar data are available for the passage of the second warm front at the SOUSY site. Figures 4a–d show contours of the radar reflectivity, the vertical velocity, the magnitude of the horizontal velocity, and a schematic representation of the structure of a front taken from Palmén and Newton (1969).

The fact that the VHF radar sees the frontal structure so clearly is due to its sensitivity to thermal stratification in the atmosphere (Green and Gage, 1980; Rastogi and Röttger, 1982) as we have already discussed. The schematic in Fig. 4d can be compared to the reflectivity contours in Fig. 4a. Not only is the comparison quite good in terms of the ability of the radar in locating the position of the front, but the schematic helps to show the temperature gradients that are associated with the increases in reflected power. Figure 4b shows the area of ascent in the warm sector of the front and the area of subsidence in the cold sector. At the time between 1800 and 2300 UT a fingered structure in the vertical velocity field is present immediately ahead of and in the area of the juncture of the warm frontal surface and the tropopause bound-

FIG. 5. a) Reflectivity contours for a warm-frontal passage observed with the SOUSY-VHF-radar during February 1982. Shading and contour levels are the same as in Fig. 4a. The crosshairs show the position of the tropopause reported by the radiosonde station at Hanover, 50 km from the site of the radar. b) Pressure-time cross-section of the potential temperature measured by the Hanover radiosonde during the period corresponding to the data in Fig. 5a. The contour interval is 5 K in the troposphere. Above 350 K isotherm, the contour interval was increased to 10 K. c) Wind vectors measured by the radar as a function of time and height. The reference scale and directions are shown at the lower left-hand corner.

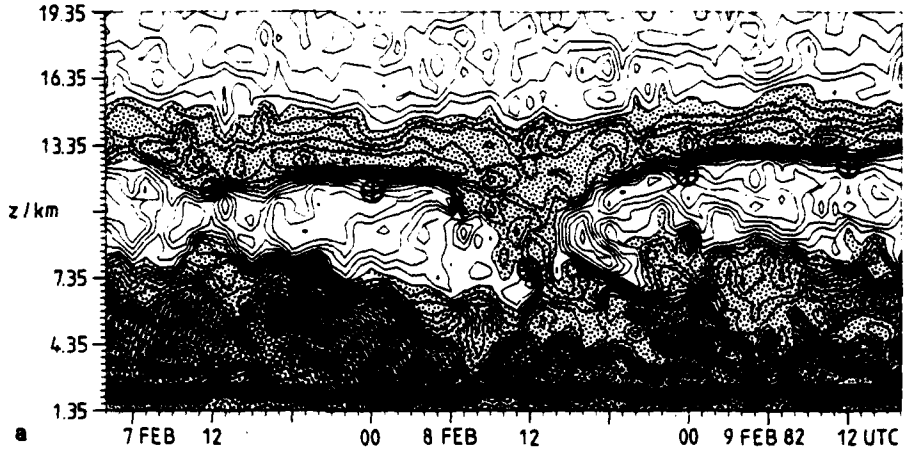
19.35
16.35
13.35
z / km
7.35
4.35
1.35
7 FEB 12 00 8 FEB 12 00 9 FEB 82 12 UTC

a

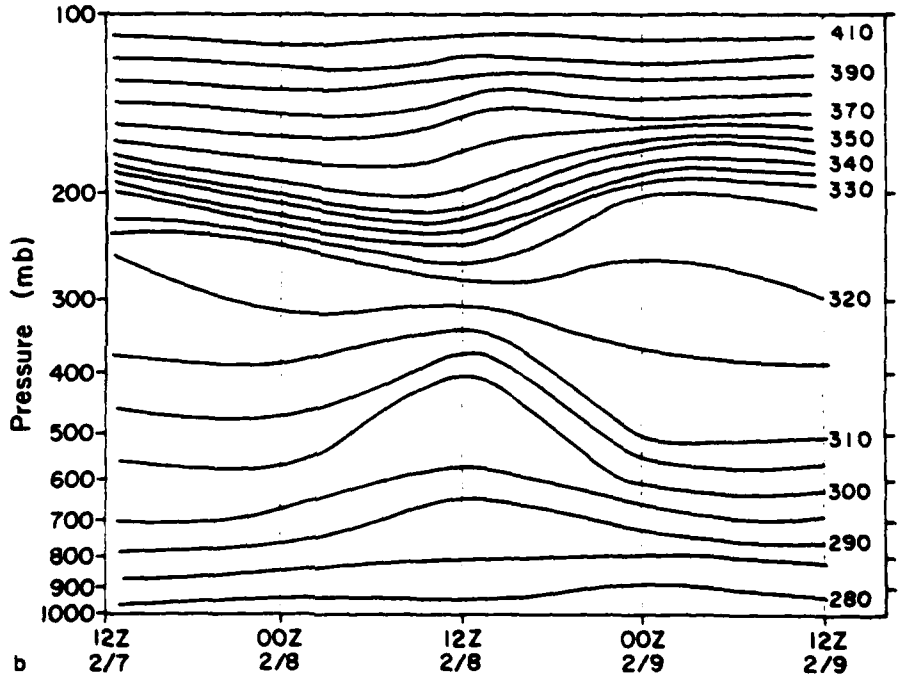
100
200
300
400
500
600
700
800
900
1000
Pressure (mb)
410
390
370
350
340
330
320
310
300
290
280
12Z 2/7
00Z 2/8
12Z 2/8
00Z 2/9
12Z 2/9

b

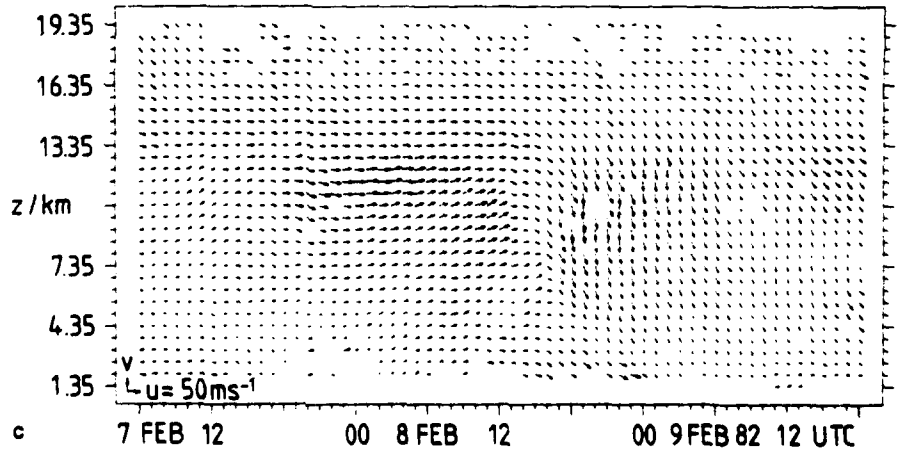
19.35
16.35
13.35
z / km
7.35
4.35
1.35
u= 50ms⁻¹
7 FEB 12 00 8 FEB 12 00 9 FEB 82 12 UTC

c

ary. There is an intrusion of stratospheric air at 2000 UT. The fingered structure associated with this event is reminiscent of the tropopause folds responsible for mixing that have been observed and discussed by Shapiro (1974, 1978).

It has to be admitted, however, that the vertical velocities measured with the radar may be contaminated by a small contribution due to the horizontal wind, if the refractive index structures are inclined to the horizontal. This is a typical feature of frontal systems and also will occur during strong gravity wave activity, e.g., lee waves. This effect can be compensated for by measuring the inclination angle with the spaced antenna set-up and applying a correction to the vertical velocities (see Appendix in Röttger, 1981c).

All the data were measured during a period of only 12 min on the full hour during the frontal passage. Thus, the vertical velocities shown in Fig. 4 are the averages for the 12 min periods and may not be representative of the conditions throughout the hour. However, the overall velocity fields are downward in the cold air and upward in the warm air. This is consistent with the expected pattern. Also, although we cannot comment on the variability in the fingered structure, there is no doubt that it is present.

The horizontal velocity cross section in Fig. 4c is very similar to the schematic structure of the winds shown in Fig. 4d. The data in the heavy stippled area in Fig. 4c have been omitted because the signal was undersampled during this particular series of observations. The radiosonde data for this period indicate a wind maximum in this region, in agreement with the schematic of Fig. 4d.

Röttger and Schmidt (1981) used the horizontal wind vector data measured by the radar to calculate the horizontal temperature gradients from the thermal wind relation. In general, good agreement between the derived and observed values was found in the height region between 700 mb and 300 mb. However, Shapiro (1974) showed that the geostrophic relation, and the thermal wind relation that it implies, can be found to explain the balance near frontal zones in a fortuitous manner. It may be that the balance is only apparent since two large gradient wind terms cancel each other. The high time resolution measurements that are possible with the VHF radar, such as those shown in Figs. 4 and 5, make it possible to get a better estimate of the peak wind associated with a jet stream than is possible with radiosondes launched every 12 h. Also, the areas of jet-stream generated turbulence can be located. Further radar observations of jet streams and their mesoscale variability have been made by Gage and Clark (1978), and Rüster and Czechowsky (1980).

Figures 5a–c show data taken with the SOUSY radar during a warm frontal passage on 8 February 1982. Figure 5a represents the contours of reflectivity, with darker shading indicating stronger echoes. The pattern is very similar to that seen in Fig. 4a. The circles with crosses are the tropopause heights reported by the Hanover radiosonde station, 50 km from the site of the radar. A large gradient in radar reflectivity is evident at the height where the tropopause occurs. At 1200 UT on 8 February, the tropopause is almost 4 km lower than reported at 0000 UT due to the passage of the warm front, and there is good agreement between the radar and radiosonde observations. The time-pressure cross-section of potential temperature at Hanover for the same period is shown in Fig. 5b for comparison with the radar reflectivities. The position of the frontal boundary is defined by the 300–310 K isotherms between 1200 UT (Z) on 8 February and 0000 UT on 9 February. Figure 5c shows the horizontal wind vectors measured by the radar as a function of height and time. The wind shift from roughly westerly on the cold side to northerly winds on the warm side of the front can be seen. The jet core passes the radar at 1700 UT on 8 February and is located at 10 km ASL. These observations are described in more detail by Larsen and Röttger (1982). The comparison between the radar and radiosonde data for this particular case not only points out the agreement between the two but also shows the details in the frontal structure that are missed by the 12 h radiosonde ascents.

The results of the observation of the frontal passage are only preliminary. The mixing between the stratosphere and troposphere will be investigated by analyzing cross sections of potential vorticity and potential temperature as suggested by Danielsen (1968) and comparing that to the vertical velocity data available. Radiosonde data also will be used to check the thermal wind relation more carefully. Finally, the position of the front can be determined based on radiosonde data and this can be compared to the position determined from the radar reflectivity. The good time resolution and height resolution of the radars may help to improve our understanding of the mixing of air that is part of the damping process for the frontal system, as well as providing a new tool for forecasting on shorter time scales (Röttger, 1981b). The vertical velocity measurements also should improve our understanding of how precipitation develops in association with the frontal structure. The combination of the radiosonde data and the Doppler radar data is particularly powerful for studying the interaction of the synoptic scale and the mesoscale.

5. Turbulence in the atmospheric mesoscale

Most of the large radar facilities capable of measuring winds throughout the troposphere and in the lower stratosphere were originally designed with other purposes in mind. Though meteorological research is being carried out at most of these facilities, only the SOUSY-VHF-radar, the Platteville radar, the Sunset radar (Green and Gage, 1980), and the Poker Flat MST radar (Balsley *et al.*, 1980) are being operated in a mode dedicated to observation of the atmosphere. Of these, the Poker Flat radar is unique in that it has been in operation continuously since the latter part of 1978, obtaining one complete profile every 4 min with a 2.2 km height resolution. This unique data set is ideal for investigations of atmospheric dynamics at both long and short time scales. At the present time the Platteville radar also is operating in a continuous mode as part of an effort by the Wave Propagation Laboratory of NOAA to establish a mesoscale prediction network (Strauch *et al.*, 1982), but the data it is providing are not as detailed. The system will eventually include three VHF radars located in a triangle around Denver, Colo., and will provide wind profiles in the troposphere in an operational mode similar to that of the Poker Flat facility. The WPL system will be described in more detail in a later section.

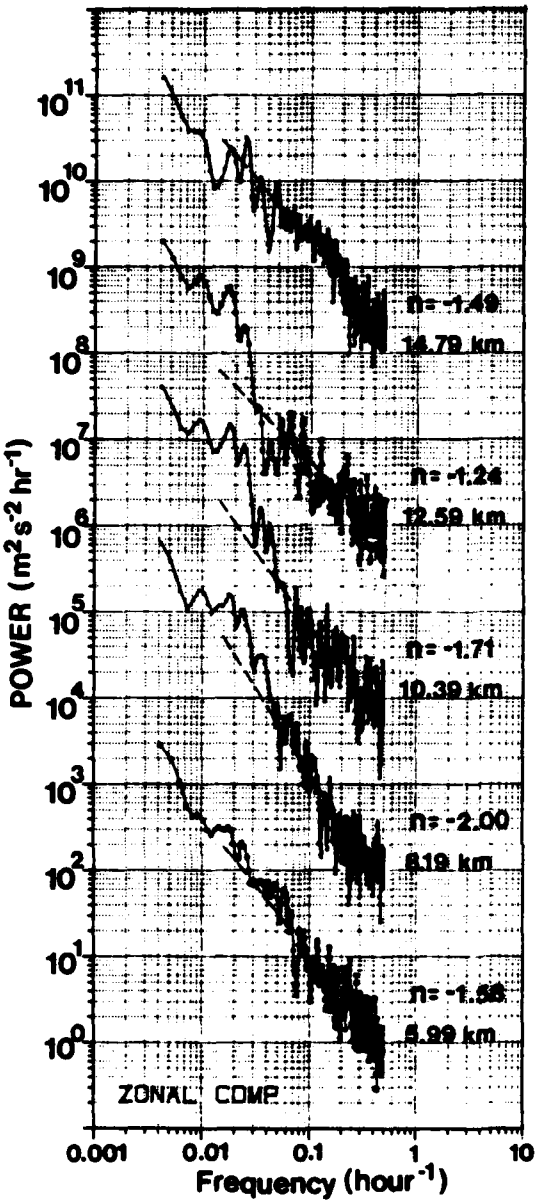

FIG. 6. Power spectra calculated from a 40-day series of wind measurements made with the Poker Flat, Alaska, MST radar. Each successive curve has been multiplied by a factor of 100. The left-hand scale is correct for the spectrum at a 5.99 km altitude. A curve of the form $P = P_0(f/f_0)^n$ was fit to the spectrum at each height, and the value of n is indicated next to each curve. The average value of the slope is $n = 1.602 \pm 0.250$.

Larsen *et al.* (1982) used the Poker Flat horizontal winds for a 40-day period from 25 February to 5 April 1979 to investigate turbulence in the mesoscale. Wind data were available on a nearly continuous basis at heights ranging from 5.99 km to 14.69 km at 2.2 km intervals. The resulting spectra for the zonal wind component are shown in Fig. 6. Corresponding to each height is the spectral index n which was determined

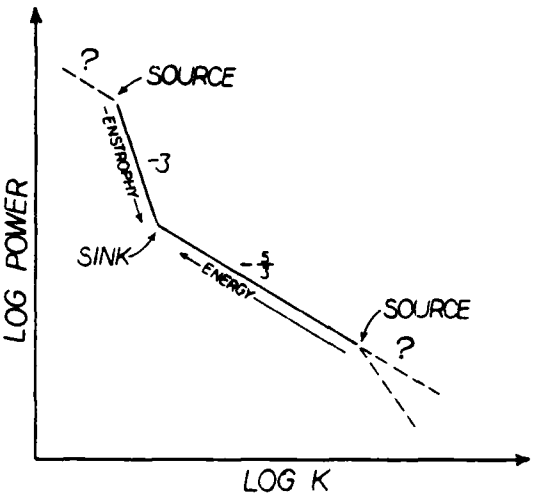

FIG. 7. Schematic representation of the energy and enstrophy flow if the $-5/3$ slope derived from the data in Fig. 6 is representative of 2-dimensional rather than 3-dimensional turbulence. The source at high wave numbers could be due to convection or small-scale wave energy generated by shear instabilities.

by least-squares fitting a power law of the form

$$P(f) = P_0(f/f_0)^n$$

to each of the spectra. Here f_0 is a reference frequency corresponding to the point in the spectrum where the power is P_0. The average value of n was found to be 1.602 ± 0.25, very close to a value of $-5/3$. The spectra for the meridional wind component are not shown but were very similar and had the same spectral index.

Gage (1979) reviewed the results from diverse studies of turbulence at scales from a few hours to a few days and pointed out that a common thread was the finding of a $-5/3$ power law. Most, though not all, of these studies used data in the frequency domain. However, if the Taylor hypothesis is valid so that eddies can be considered to be moving with the mean wind over the sampling period, then a $k^{-5/3}$ power law is implied. Gage further postulated that at these large scales the turbulence is 2-dimensional rather than 3-dimensional. Following Kraichnan's (1967) theory, this would imply that a source of energy exists at small scales and energy is transferred up the spectrum toward larger scales in what has been termed a "red cascade."

Lilly (1982) has expanded the theory of 2-dimensional turbulence at these scales and has shown that 3-dimensional internal wave structure can coexist with 2-dimensional turbulent eddies relatively independent of the other. Lilly pointed out that an energy source due to convection or small-scale shear instabilities would occur in a 3-dimensional range but could leak enough energy into the 2-dimensional range to account for the observations. The energy and enstrophy flow are shown schematically in Fig. 7. At scales larger than 1000 km a k^{-3} enstrophy cascade range of 2-dimensional turbulence exists (see, e.g., Julian *et al.*, 1970).

Van Zandt (1982) has proposed that the observations also can be explained if the spectra are due to a universal Garrett-

Munk type spectrum, which is well known in the oceans. The implication would be that a gravity wave spectrum exists with interaction between different wavenumbers. The direction of the energy cascade would be the same as that of the 2-dimensional turbulence, but the dynamics would be inherently 3-dimensional. The question of which view is correct still needs to be resolved.

The spectra in Fig. 6 show a pronounced peak at a period of 50 h, very close to the 51 h period of the wavenumber 3 mode, two-day Rossby wave (see Salby, 1981). Salby's (1981) calculations indicate that the wave should be observable, though with a small amplitude, at latitudes corresponding to that of Poker Flat and for the time of year of the observations. Yet, it is clearly a significant feature of the wind variations during the observation period.

6. An examination of objective analysis schemes

The method used for interpolating observed data, usually from radiosondes, to a regularly spaced grid suitable for input to a numerical model, is termed objective analysis. The various schemes used for this process are designed to operate under two constraints. First, the value calculated for a given grid point should be representative of the true value of the parameter such as height of an isobar, temperature, or wind, at that grid point, corresponding to a scale size no smaller than the smallest scale that can be resolved by the model. Second, the derived values have to provide a balanced field to minimize the generation of spurious oscillations that can create errors in a numerical integration (see, e.g., Kruger, 1969). The first constraint is usually handled by providing a good initial guess of the value at the grid point and weighting it with observed values within a predetermined radius of influence of the grid point. This approach provides reasonable values in data-sparse areas and smooths out errors due to observational inaccuracies or oscillations, with characteristic scales smaller than the numerical model can handle. The second constraint can be met by requiring that the derived wind and height fields are in geostrophic balance. This is the simplest approach. A more complex approach is to require that the balance equation should be satisfied or that all the derived fields can be described by the normal modes of the numerical model (Daley, 1981).

A check on a scheme that requires geostrophy for balance would be to compare the geostrophic wind calculated from the derived height field to the actual geostrophic wind if a good estimate of that quantity is available, but it has been difficult to do in practice. Therefore, more elaborate schemes have been devised to test the various objective analysis schemes. Often the test has been a comparison of the output after application of the analysis procedure to a subjective analysis of the same data (Kruger, 1969; Otto-Bliesner *et al.*, 1977).

Larsen *et al.* (1981) used the data base from the Poker Flat radar described in the previous section to evaluate the Cressman (1959) and Gandin (1963) objective analysis methods. These schemes use a parabolic and a Gaussian weighting function, respectively, and are univariate. The weighting is

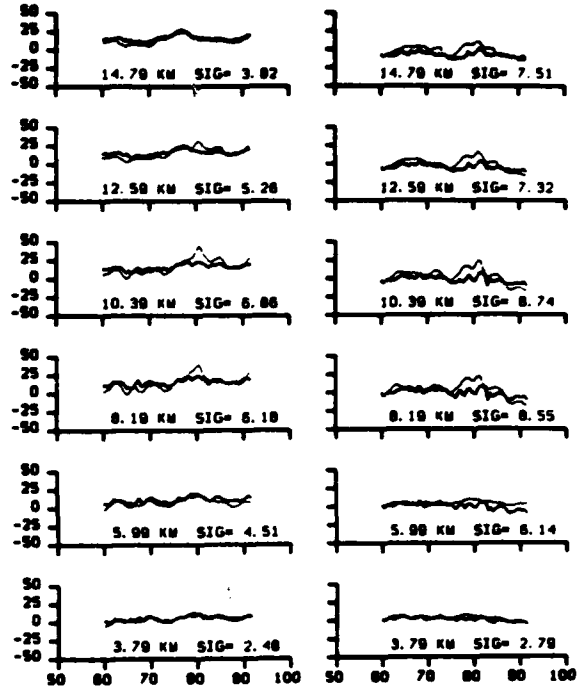

FIG. 8. Comparison of the radar winds averaged over 48 h centered on the time of radiosonde ascents (light line) and the geostrophic wind calculated from a grid of height data for isobaric surfaces (heavy line). The geopotential-height grid was calculated by applying the Cressman objective analysis scheme to the available radiosonde data from five stations located near the Poker Flat MST radar. The left-hand scale is velocity in m/s. The six curves on the right are for the meridional wind component. The quantity "sigma" is the rms difference between the two curves. The horizontal scale is Julian days.

only a function of radial distance from the grid point. The geostrophic wind calculated from the gridded values of the height field was compared to averages of the radar wind data over various time intervals centered on 0000 GMT and 1200 GMT, the times of the standard NWS radiosonde ascents. The rationale was that averaging of the 4 min wind measurements over periods of several hours should produce a good estimate of the balanced wind component, though the appropriate averaging interval had to be determined by trial and error. Since the radar provides many profiles in a 12 h period, as opposed to only one by the radiosonde, these can be averaged to produce a better estimate of the wind without the influence of meteorological noise.

The objective analysis schemes tested are the simplest ones that are available. However, the results have implications for the more complex multivariate optimum-interpolation schemes, since additional data for the interpolation scheme are gained by relating the height and wind fields through the geostrophic relation (Williamson *et al.*, 1981; Schlatter, 1975; Rutherford, 1972). The gradient wind relation is generally not used since it makes the problem nonlinear and thus more difficult to solve.

An example of the result of the comparison is shown in Fig. 8. The thin line represents a 48 h average of the radar

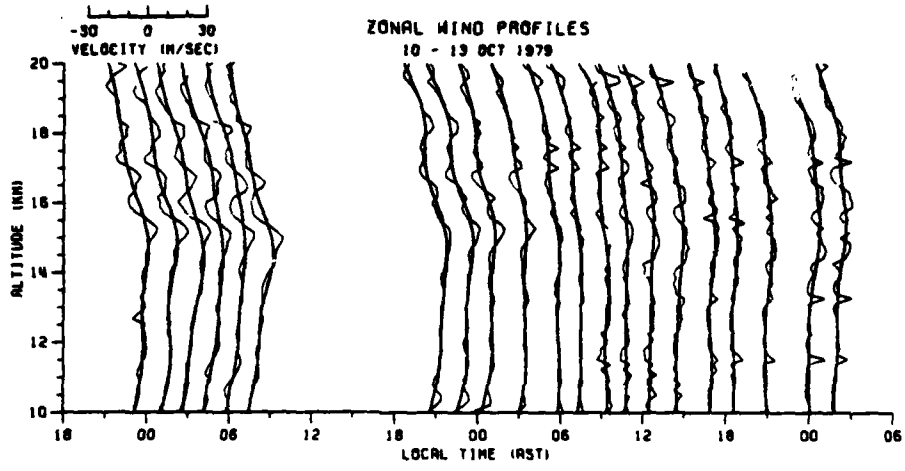

FIG. 9. Mean zonal wind profile and perturbations during a 48 h period measured with the Arecibo Observatory 430 MHz radar. Waves with a vertical wavelength of 1–2 km are present and a downward phase progression can be seen, at least in the first 6 h. A more detailed analysis has revealed that the wave period is close to 4 days.

winds measured every 4 min. The heavy line is the geostrophic wind determined by the application of the Cressman method with a radius of influence of 750 km to height data from five radiosonde stations surrounding the Poker Flat site. The results of the study show that there is essentially no difference between the Cressman and Gandin methods. For both of these schemes the optimum radius of influence is smaller than that conventionally used. For the Cressman method a commonly used radius is a little over 2000 km. The comparison indicated an optimum value of 750 km. Also, the Cressman analysis is usually applied in a series of successive scans in which the radius of influence is successively decreased to improve the estimate of variations at smaller scales. The comparison with the radar data indicated that this produces a result slightly poorer than a single scan with the optimum radius of 750 km. Finally, the difference between the geostrophic wind component and the radar wind component decreased rapidly as the averaging interval was increased out to 48 h. Beyond 48 h of averaging the difference decreased, but only slightly.

There is great potential for more studies of this kind that rely on the ability of the radar to provide good estimates of the winds free of the errors due to short term variability of the atmosphere. This type of study is not only important with regard to research but also will be important in assessing possible benefits of operational use of the radars. An investigation of a multivariate scheme using the radar and radiosonde data is planned for the near future.

7. Detection of tropical waves and tides

Wind measurements made at the Arecibo Observatory by Sato and Woodman (1982) using the 430 MHz radar always show perturbations in the vertical profile with a scale size of ~1 km. The perturbations usually only undergo one complete oscillation in the vertical direction, so it is difficult to speak of a wave train. There is very little vertical phase progression over a period of a few hours. Observations over a period of 48 h have shown that there is indeed vertical phase progression, but on a scale of several days. This is shown in Fig. 9, which presents a series of wind profiles from that experiment. It was determined that the period of the wave was likely to be four or five days. However, the observational period was too short to determine it accurately. Fukao *et al.* (1981) have seen the same kind of wave at Jicamarca, Peru, during a 48 h observation period. They also estimated the period of the wave to be between four and five days.

The period and the wavelength are characteristic of a mixed Rossby-gravity wave, which is an important part of the dynamics at low latitudes (see, e.g., Holton, 1975). Since the period is of the order of days, the high time resolution of the radars is not really necessary to observe the wave, but the high spatial resolution is, since the vertical wavelength is so small. Cadet and Teitelbaum (1979) detected the mixed Rossby-gravity wave in data taken during the GATE experiment. It was possible to resolve the wave structure because radars with high spatial resolution had been used to track the rawinsondes launched during the experiment. With the radars it will be possible to observe the waves on a more routine basis.

The ability of the VHF radars to measure vertical velocities on a routine basis also can have important consequences for tropical meteorology. Little work has been done in this regard to date, but it should be possible to improve our understanding of the interaction of the waves in the easterlies and the convection that they trigger on the cloud cluster scales. Radars operating at meter wavelengths can measure both the vertical velocities within the clouds and the centimeter per second vertical velocities associated with the waves. Over longer observation intervals, the annual transport of mass across the tropopause boundary associated with the tropical branch of the Hadley cell also could be studied.

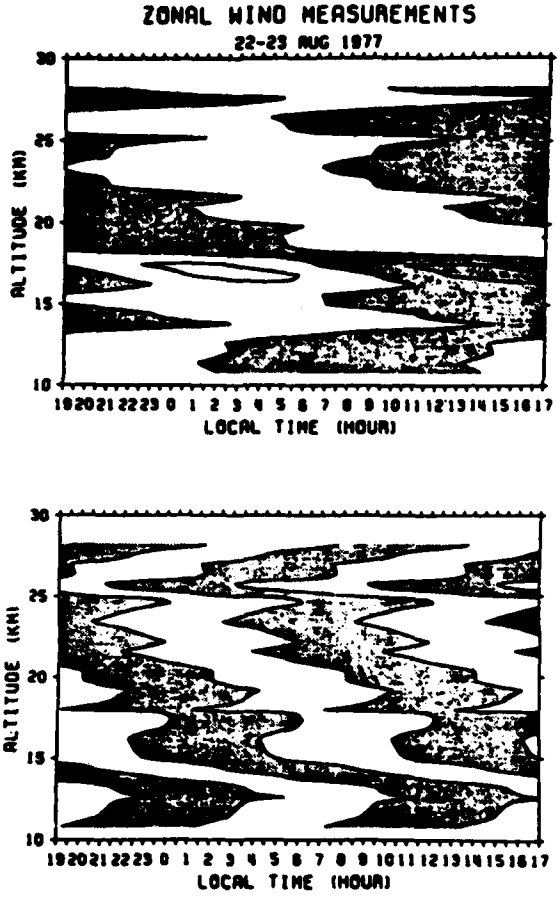

FIG. 10. Diurnal and semi-diurnal tidal components measured by Fukao *et al.* (1980) at Arecibo, Puerto Rico. The velocity time series were filtered to exclude everything but the particular frequency component of interest. The tidal components show downward phase progression and upward energy propagation in the lower stratosphere.

Fukao *et al.* (1980) have used the Arecibo radar to study the dynamics of the diurnal and semidiurnal tidal components. Figure 10 shows a time series over a period of 24 h which has been filtered to exclude frequency components other than those of the tides. The phase progression indicates that the source of energy for the diurnal tide is in the troposphere and is in agreement with the results of Wallace and Tadd (1974), whose investigation based on radiosonde data showed that the strong diurnal component seen in the troposphere at low latitudes is not the classical tidal component. Rather, it is driven by the interaction of the flow with the orography or some other input of energy in the troposphere. Fukao *et al.* (1978) have observed the semidiurnal and diurnal tides at Jicamarca, Peru, but they found that the semidiurnal tide dominated in the troposphere and the diurnal tide could only be seen in the stratosphere. This may be an indication that the energy source for the tropospheric diurnal tide seen at Arecibo is very localized.

8. The Wave Propagation Laboratory profiler

The first real attempt at operational use of the UHF/VHF Doppler radar wind measurements is as part of a system developed by the Wave Propagation Laboratory (WPL) of NOAA. The system is designed to be competitive with the NWS radiosonde (Hogg *et al.*, 1980; Strauch, 1981; Strauch *et al.*, 1982). The prototype Profiler consists of a dual wavelength radiometer that measures total precipitable water vapor content and vapor profiles, a microwave radiometer that provides temperature profiles, a UHF radar for wind profiling, and a VHF radar that determines the height of the tropopause and provides wind information. The standard surface measurements also are taken by the system. The drawbacks of the system are that the microwave technique does not provide a detailed profile of the water vapor content of the atmosphere as a function of height. However, the total precipitable water vapor measurements have been found to be in good agreement with the same quantity measured by radiosonde (Hogg *et al.*, 1980). The temperature profile determined by using the microwave radiometer is far less detailed than that of the radiosonde, but it may be that the resolution of the radiometer measurement will be sufficient for synoptic forecasting.

The system has been designed to provide data roughly every half hour. Most of the components of the system are located at the airport in Denver, Colo., and the VHF radar is located at Platteville, Colo. At the present time it mainly provides data on the height of the tropopause and other inversions. This information was found to be valuable in increasing the accuracy of the radiometer temperature profiles (Strauch, 1981). Eventually three more VHF radars for wind profiling are planned as part of the PROFS (Prototype Regional Observing and Forecasting Service) program. These radars will be located in a triangle around Denver, about 150 to 200 km from the airport site. It is expected that data from the total system will be used to increase flight safety, decrease airplane fuel consumption, and significantly improve short-term forecasting.

As the present review indicates, the UHF and VHF radars have mostly been used as tools for research in the past, although the potential for operational use has been realized for a number of years. The WPL effort is the first dedicated evaluation of the synoptic potential of the radar wind measurement system. The radar by itself could never replace the radiosonde, since there are no means of determining the thermodynamic variables from the radar measurements. The addition of the radiometer temperature measurements to the radar-derived wind profiles makes the system a much more serious competitor for the radiosonde. However, the water vapor measurements are still not detailed enough to provide adequate information even for synoptic-scale forecasting.

Regardless of whether the radar systems replace the radiosonde network, they have certain characteristics that would at least argue for an eventual fusion of the two types of networks. The radars provide very reliable measurements and little routine maintenance is needed. The wind data can be processed completely automatically, and the measurements can be made regardless of the state of the weather (Gage and Balsley, 1978; Hogg *et al.*, 1980). Thus, the system is ideal for operation in remote places where few data are available other-

wise. In fact, Balsley and Gage (1980) have proposed that a series of buoys equipped with Yagi antennas could provide wind measurements up to the tropopause level. The data would be processed onboard and sent via satellite to the data collection center. Possible problems with this idea are that there might be contamination of the wind data due to sea clutter detected in the side lobes, and the antenna area will necessarily have to be rather small. However, if these problems can be solved, such a system would give a tremendous improvement in the data coverage over the oceans, where so few data are available now.

9. Conclusion

We have presented a sample of recent results obtained by applying the UHF/VHF Doppler radar technique to synoptic research. The review is by no means exhaustive but should provide a general idea of the direction of research in the field so far. There is little doubt that the radars will become an important research tool for studies of synoptic scale dynamics. The improved temporal resolution along with the capability of vertical velocity measurements is opening new avenues of inquiry. The characteristics of the radars seem to be particularly suited to investigations of the interaction between the synoptic scale and the mesoscale, as the results covered in this review indicate.

There appears to be a great potential for operational use of the radar measurements. What direction the development of the systems will take is still not quite certain, but the efforts of the Wave Propagation Laboratory of NOAA in testing their Profiler system will help to determine the course. Further testing of the radar/radiometer measurement technique for synoptic purposes is needed, not only to determine if the functions of the radiosonde network can be replaced or augmented by this technique, but also to evaluate the possibility of using the radar system as a data gathering technique for remote areas.

Acknowledgments. Both of us would like to thank Ted Cress of AFOSR and Ron Taylor of NSF for suggesting the idea for this review. One of us (MFL) would like to thank the Air Force Office of Scientific Research for providing support under grant AFOSR-80-0020 while this paper was being written.

References

Balsley, B. B., and D. T. Farley, 1976: Auroral zone winds detected near the tropopause with the Chatanika UHF Doppler radar. *Geophys. Res. Lett.*, 3, 525–528.

——, and K. S. Gage, 1980: The MST radar technique: Potential for middle atmospheric studies. *Pure Appl. Geophys.*, **118**, 452–493.

——, and ——, 1982: On the use of radars for operational wind profiling. *Bull. Am. Meteorol. Soc.*, **63**, 00 00.

——, W. L. Ecklund, D. A. Carter, and P. E. Johnston, 1980: The MST radar at Poker Flat, Alaska. *Radio Sci.*, **15**, 213–224.

——, J. L. Green, W. L. Ecklund, W. L. Clark, R. G. Strauch, and A. C. Riddle, 1981: Joint observations of gravity wave activity in vertical winds in the troposphere and lower stratosphere over a 63 km baseline obtained with clear-air VHF radars at Platteville and Sunset, Colorado. *Preprints, 20th Conference on Radar Meteorology (Boston)*, AMS, Boston, pp. 110–115.

Battan, L. J., 1973: *Radar Observation of the Atmosphere.* The University of Chicago Press, Chicago, 324 pp.

Briggs, B. H., 1980: Radar observations of atmospheric winds and turbulence: A comparison of techniques. *J. Atmos. Terr. Phys.*, **42**, 823–833.

Cadet, D., and H. Teitelbaum, 1979: Observational evidence of inertia-gravity waves in the tropical stratosphere. *J. Atmos. Sci.*, **36**, 893–907.

Cressman, G. P., 1959: An operational objective analysis system. *Mon. Wea. Rev.*, **87**, 367–374.

Daley, R., 1981: Normal mode initialization. *Rev. Geophys. Space Phys.*, **19**, 450–468.

Danielsen, E. F., 1968: Stratospheric-tropospheric exchange based on radioactivity, ozone, and potential vorticity. *J. Atmos. Sci.*, **25**, 502–518.

Doviak, R. J., D. S. Zrnic, and D. S. Sirmans, 1979: Doppler weather radar. *Proc. IEEE.*, **67**, 1522–1553.

Ecklund, W. L., K. S. Gage, and A. C. Riddle, 1981a: Gravity wave activity in vertical winds observed by the Poker Flat MST radar. *Geophys. Res. Lett.*, **8**, 285–288.

——, ——, and B. B. Balsley, 1981b: A comparison of vertical wind variability observed with the Platteville VHF radar and local weather conditions. *Preprints, 20th Conference on Radar Meteorology (Boston)*, AMS, Boston, pp. 104–109.

Farley, D. T., B. B. Balsley, W. E. Swartz, and C. La Hoz, 1979: Tropical winds measured by the Arecibo radar. *J. Appl. Meteorol.*, **18**, 227–230.

Fukao, S., S. Kato, S. Yokoi, R. M. Harper, R. F. Woodman, and W. E. Gordon, 1978: One full-day radar measurement of lower stratospheric winds over Jicamarca. *J. Atmos. Terr. Phys.*, **40**, 1331–1337.

——, T. Sato, N. Yamasaki, R. M. Harper, and S. Kato, 1980: Radar measurement of tidal winds at stratospheric heights over Arecibo. *J. Atmos. Sci.*, **37**, 2540–2544.

——, K. Aoki, K. Wakasugi, T. Tsuda, S. Kato, and D. A. Fleisch, 1981: Some further results on the lower stratospheric winds and waves over Jicamarca. *J. Atmos. Terr. Phys.*, **43**, 649–661.

Gage, K. S., 1979: Evidence for a $k^{-5/3}$ law inertial range in mesoscale two-dimensional turbulence. *J. Atmos. Sci.*, **36**, 1950–1954.

——, and B. B. Balsley, 1978: Doppler radar probing of the clear atmosphere. *Bull. Am. Meteorol. Soc.*, **59**, 1074–1093.

——, and B. B. Balsley, 1978: Doppler radar probing of the clear atmosphere. *Bull. Am. Meteorol. Soc.*, **59**, 1074–1093.

——, and W. L. Clark, 1978: Mesoscale variability of jet stream winds observed by the Sunset VHF Doppler radar. *J. Appl. Meteorol.*, **17**, 1412–1416.

Gandin, L. S., 1963: *Objective Analysis of Meteorological Fields*, 242 pp. Translated from the Russian (1965) by the Israel Program for Scientific Translations Ltd., Jerusalem.

Green, J. L., and K. S. Gage, 1980: Observations of stable layers in the troposphere and stratosphere using VHF radar. *Radio Sci.*, **15**, 395–406.

Harper, R. M., and W. E. Gordon, 1980: A review of radar studies of the middle atmosphere. *Radio Sci.*, **15**, 195–211.

Hogg, D. C., F. O. Guiraud, C. G. Little, R. G. Strauch, M. T. Decker, and E. R. Westwater, 1980: Design of a ground-based remote sensing system using radio wavelengths to profile lower atmospheric winds, temperature, and humidity. In *Remote Sensing of Atmospheric and Oceans*, Academic Press, New York, pp. 313–364.

Holton, J. R. 1975: *The Dynamic Meteorology of the Stratosphere and Mesosphere. Meteorol. Monogr.* (37), AMS, Boston, 218 pp.

——, 1981: Tropospheric-stratospheric coupling, chemical and dy-

namical. In *Handbook for MAP*, edited by C. F. Sechrist, Jr., SCOSTEP Secretariat, University of Illinois, Urbana, pp. 5–13.

Julian, P. R., W. M. Washington, L. Hembree, and C. Ridley, 1970: On the spectral distribution of large-scale atmospheric kinetic energy. *J. Atmos. Sci.*, **27**, 376–387.

Klostermeyer, J., 1981: MST radars: Advanced tools for gravity wave studies. *Nature*, **292**, 107–108.

Kraichnan, R. H., 1967: Inertial ranges in two-dimensional turbulence. *Phys. Fluids*, **10**, 1417–1423.

Kruger, H. B., 1969: General and special approaches to the problem of objective analysis of meteorological variables. *Quart. J. Roy. Meteorol. Soc.*, **95**, 21–39.

Larsen, M. F., and J. Röttger, 1982: Analysis of VHF radar wind and reflectivities during a frontal passage. School of Electrical Engineering, Cornell University, Ithaca, N.Y.

——, M. C. Kelley, and D. T. Farley, 1981: Report on the analysis of data from the NOAA/Alaskan MST radar system. Second Progress Report, School of Electrical Engineering, Cornell University, Ithaca, N.Y., 38 pp.

——, ——, and K. S. Gage, 1982: Turbulence spectra in the upper troposphere and lower stratosphere at periods between 2 hours and 40 days. *J. Atmos. Sci.*, **39**, 1035–1041.

Lhermitte, R. M., and D. Atlas, 1963: Doppler fall speed and particle growth in stratiform precipitation. *Proceedings, 10th Weather Radar Conference*, Washington, D.C., 22–25 April 1963, AMS, Boston, pp. 297–302.

Lilly, D. K., 1982: Stratified turbulence and the mesoscale variability of the atmosphere. Submitted to *J. Atmos. Sci.*

Otto-Bliesner, B., D. P. Baumhefner, T. W. Schlatter, and R. Bleck, 1977: A comparison of several meteorological analysis schemes over a data-rich region. *Mon. Wea. Rev.*, **105**, 1083–1091.

Palmén, E., and C. W. Newton, 1969: *Atmospheric Circulation Systems: Their Structure and Interpretation*. Academic Press, New York, 603 pp.

Rastogi, P. K., and J. Röttger, 1982: VHF radar observations of coherent reflections in the vicinity of the tropopause. *J. Atmos. Terr. Phys.*, in press.

Röttger, J., 1979: VHF radar observations of a frontal passage. *J. Appl. Meteorol.*, **18**, 85–91.

——, 1980: Structure and dynamics of the stratosphere and mesosphere revealed by VHF radar investigations. *Pure Appl. Geophys.*, **118**, 494–527.

——, 1981a: Investigations of lower and middle atmospheric dynamics with spaced antennas drifts. *J. Atmos. Terr. Phys.*, **43**, 277–292.

——, 1981b: The capabilities of VHF radars for meteorological observations. In *Nowcasting: Mesoscale Observations and Short-Range Prediction*, European Space Agency, Paris, pp. 143–148.

——, 1981c: Wind variability in the stratosphere deduced from spaced antenna VHF radar measurements. *Preprints, 20th Conference on Radar Meteorology (Boston)*, AMS, Boston, pp. 22–29.

——, and G. Schmidt, 1981: Characteristics of frontal zones determined from spaced antenna VHF radar observations. *Preprints, 20th Conference on Radar Meteorology, (Boston)*, AMS, Boston, pp. 30–37.

——, and R. A. Vincent, 1978: VHF radar studies of tropospheric velocities and irregularities using spaced antenna techniques. *Geophys. Res. Lett.*, **5**, 917–920.

Rüster, R., and P. Czechowsky, 1980: VHF radar measurements during a jetstream passage. *Radio Sci.*, **15**, 363–369.

Rutherford, I. D., 1972: Data assimilation by statistical interpolation of forecast error fields. *J. Atmos. Sci.*, **29**, 809–815.

Salby, M. L., 1981: The 2-day wave in the middle atmosphere: Observations and theory. *J. Geophys. Res.*, **86**, 9654–9660.

Sato, T., and R. F. Woodman, 1982: High altitude-resolution observations of upper-tropospheric and lower-stratospheric winds and waves by the Arecibo 430 MHz radar. Submitted to *J. Atmos. Sci.*

Schlatter, T. W., 1975: Some experiments with a multivariate statistical objective analysis scheme. *Mon. Wea. Rev.*, **103**, 246–257.

Shapiro, M. A., 1974: A multiple structured frontal zone-jet stream system revealed by meteorologically instrumented aircraft. *Mon. Wea. Rev.*, **102**, 244–253.

——, 1978: Further evidence of the mesoscale and turbulent structure of upper level jet stream-frontal zone systems. *Mon. Wea. Rev.*, **106**, 1100–1111.

Strauch, R. G., 1981: Radar measurement of tropospheric wind profiles. *Preprints, 20th Conference on Radar Meteorology (Boston)*, AMS, Boston, pp. 430–434.

——, M. T. Decker, and D. C. Hogg, 1982: An automatic profiler of the troposphere. *Preprints, AIAA 20th Aerospace Sciences Meeting (Orlando, Fla.)*, American Institute of Aeronautics and Astronautics, New York.

Van Zandt, T. E., 1982: A universal spectrum of buoyancy waves in the atmosphere. *Geophys. Res. Lett.*, **9**, 575–578.

Vincent, R. A., and J. Röttger, 1980: Spaced antenna VHF radar observations of tropospheric velocities and irregularities. *Radio Sci.*, **15**, 319–335.

Wallace, J. M., and R. F. Tadd, 1974: Some further results concerning the vertical structure of atmospheric tidal motions within the lowest 30 km. *Mon. Wea. Rev.*, **102**, 795–803.

Williamson, D. L., R. G. Daley, and T. W. Schlatter, 1981: The balance between mass and wind fields resulting from multivariate optimal interpolation. *Mon. Wea. Rev.*, **109**, 2357–2376.

Wilson, D. A., and L. J. Miller, 1972: Atmospheric motion by Doppler radar. In *Remote Sensing of the Troposphere*, NOAA, Washington, D.C.

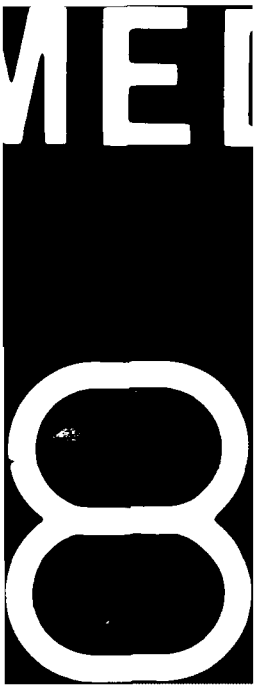
WE
8